# 1. The point-by-point response to the reviews

------------------------------------ Reviewer #1 --------------------------------------

**Review for "Hydrological effects of climate variability and vegetation dynamics on annual fluvial water balance at global large river basins"**

This paper proposed an index of climate seasonality and asynchrony to measure the mismatch of annual precipitation and evapotranspiration. The authors then assessed the impact of climate seasonality and asynchrony on the inter-annual variations of the controlling parameter within the budyko framework, and the evapotranspiration and runoff as well. This paper is well written, well-organized and easy to understand. I have several suggestions listed below to help improve the paper. I think this paper can be published if these issues are well addressed.

**Re: Thank you so much for your positive comments and valuable suggestions to improve the quality of our manuscript. According to your excellent suggestion, we have made some extensive revisions to our previous draft. All of these comments have been carefully considered and all of them have been adopted and incorporated to the revised version. In the following sections, we provide point-to-point response to the comments. We believe that the concerns from you have been fully addressed. Thanks again for your time, suggestions and comments.**

Specific comments:

Line 41: was proposed. Please carefully gone through the manuscript to reduce grammatical and punctuation errors.

**Re: Thank you for your kind comments. It has been revised. Besides, we have checked the grammar and punctuation for the revised manuscript.**

Line 114: delete therefore Line 124: were obtained

**Re: It has been done.**

Lines 145-149: You should introduce more background of the budyko framework and the budyko equations, and explain why you use the choudhury equation. For example, Zhou et al. (2015) has summarized existing budyko equations and suggests the choudhury equation is better than other equations, which can help readers better understand the budyko framework.

Zhou, S., Yu, B., Huang, Y., & Wang, G. (2015). The complementary relationship and generation of the Budyko functions. Geophysical Research Letters, 42(6), 1781-1790.

**Re: Thank you for your kind suggestion. We have added more details about the choudhury equation. The text states as follows: "The Budyko framework has been widely used in assessment of impacts of climate and vegetation variations on hydrological cycle. There are several analytical equations proposed under the Budyko framework, among which the function deduced by Choudhury (1999) and Yang et al. (2008) has been identified to perform better than other equations (Zhou et al., 2015). The function can be expressed as…"**

Line 160: by minimizing the MAE of what? Evapotranspiration or runoff? You should point out this.

**Re: It has been done. The Parameter *n* is calibrated by minimizing the MAE of runoff.**

Equation (8): Could you explain more of the physical meanings of a and b, and why you define SAI in this way.

**Re: The a and b come from an auxiliary Angle formula, which can be expressed as: "$a\sin x + b\cos x = (a^2 + b^2)^{1/2}\sin(x + \varphi)$. In the function, sinx and cosx are unit vectors, a and b are the change range of unit vectors. The $(a^2 + b^2)^{1/2}$ is the modulus of the sum of the two vectors. The $\varphi$ is the angle between the vector and horizontal axis.**

**In equation (7):**

$$\frac{P(t) - E_0(t)}{\bar{P}} = (1 - DI) + \left(\delta_P \sin\left(\frac{2\pi}{\tau}\frac{t - S_P}{12}\right) - DI\,\delta_{E_0}\sin\left(\frac{2\pi}{\tau}\frac{t - S_{E_0}}{12}\right)\right)$$

$$= (1 - DI) + \left(\delta_P \cos\frac{2\pi}{\tau}\frac{S_P}{12} - DI\delta_{E_0}\cos\frac{2\pi}{\tau}\frac{S_{E_0}}{12}\right)\sin\frac{2\pi}{\tau}\frac{t}{12} + \left(-\delta_P \sin\frac{2\pi}{\tau}\frac{S_P}{12} + DI\delta_{E_0}\sin\frac{2\pi}{\tau}\frac{S_{E_0}}{12}\right)\cos\frac{2\pi}{\tau}\frac{t}{12}$$

**This equation is similar to the auxiliary Angle formula. Therefore, we defined a** $= \left(\delta_P \cos\frac{2\pi}{\tau}\frac{S_P}{12} - DI\delta_{E_0}\cos\frac{2\pi}{\tau}\frac{S_{E_0}}{12}\right)$, **b** $= \left(-\delta_P \sin\frac{2\pi}{\tau}\frac{S_P}{12} + DI\delta_{E_0}\sin\frac{2\pi}{\tau}\frac{S_{E_0}}{12}\right)$.

**Then,**

$$\frac{P(t) - E_0(t)}{\bar{P}} = (1 - DI) + a\sin\frac{2\pi}{\tau}\frac{t}{12} + b\cos\frac{2\pi}{\tau}\frac{t}{12} = (a^2 + b^2)^{1/2}\sin\left(\frac{2\pi}{\tau}\frac{t}{12} + \varphi\right)$$

**Where,** $\varphi = \arctan(b/a)$.

Line 234: If the difference operator refers to the changes in the variables, the left and right-hand sides of equations (9a) and (9b) are not equivalent, see Yang et al. (2014) and Zhou et al. (2016). You should point out this.

Yang, H. B., D. W. Yang, and Q. F. Hu (2014), An error analysis of the Budyko hypothesis for assessing the contribution of climate change to runoff, Water Resources Research, 50, 9620–9629, doi:10.1002/2014WR015451.

Zhou, S., Yu, B., Zhang, L., Huang, Y., Pan, M., & Wang, G. (2016). A new method to partition climate and catchment effect on the mean annual runoff based on the Budyko complementary relationship. Water Resources Research, 52(9), 7163-7177.

**Re: Thank you for your kind suggestion. We have revised the equal signs to approximately equal sign. Besides, we also added more details to point out that. The text states as follow: "It is worth noting that equations (9) is derived by the first-order approximation of Taylor expansion. When the changes of $dP_e$, $dE_0$ and $dn$ are small, the error from approximation can be ignored. However, due to ignoring the higher orders of the Taylor expansion, the error will increase as the changes increase (Yang et al., 2014; Zhou et al., 2014; Yang et al., 2016)."**

Yang, Hanbo, et al. "The Regional Variation in Climate Elasticity and Climate Contribution to Runoff across China." Journal of Hydrology, vol. 517, no. 517, 2014, pp. 607–616.

Yang, H. B., D. W. Yang, and Q. F. Hu (2014), An error analysis of the Budyko hypothesis for assessing the contribution of climate change to runoff, Water Resources Research, 50, 9620–9629, doi:10.1002/2014WR015451.

Zhou, S., Yu, B., Zhang, L., Huang, Y., Pan, M., & Wang, G. (2016). A new method to partition climate and catchment effect on the mean annual runoff based on the Budyko complementary relationship. Water Resources Research, 52(9), 7163-7177.

Equation (10): If you calculate the contributions in this way, readers cannot tell whether the contribution is positive or negative. Please change the numerators to actual values instead of absoluate values.

**Re: Thank you for your kind suggestion. We have deleted the absolute value sign in Equation (10). Besides, we added a Table in the revised manuscript (Table S4 in supplement), which summarizes the contribution to *R* and *E* changes in the form of positive or negative (Shown as below). In order to make the contribution to display more intuitively, we retained the Figures 8 and 9 in the form of absolute value of contributions.**

**Table S4.** Contributions to the long-term mean changes of *R* and *E* from $P_e$, SAI, M and $E_0$ changes.

| | | Contributions to *R* changes | | | | Contributions to *E* changes | | | |
|---|---|---|---|---|---|---|---|---|---|
| ID | Basins | P | E0 | M | SSI | P | E0 | M | SSI |
| 1 | Amazon | 63.7 | -10.1 | 25.5 | -0.7 | 19.8 | 22.3 | 55.4 | -2.5 |

| | | | | | | | | | |
|---|---|---|---|---|---|---|---|---|---|
| 2 | Amur | -59.9 | -11.2 | 4.2 | 24.6 | -51.7 | 13.5 | 13.6 | 21.2 |
| 3 | Aral | -13.2 | -9.3 | -21.4 | 56.1 | 33.9 | 7.0 | -10.1 | 48.9 |
| 4 | Columbia | -69.3 | -15.5 | 4.0 | 11.2 | -44.5 | 28.1 | 11.5 | 15.9 |
| 5 | Congo | 26.2 | -8.1 | -30.8 | 34.9 | -7.8 | 10.1 | -37.7 | 44.4 |
| 6 | Danube | 17.3 | -19.0 | 59.4 | -4.4 | 17.8 | 18.9 | 51.1 | 12.2 |
| 7 | Indigirka | -54.3 | -6.5 | 30.2 | -9.0 | -21.4 | 11.2 | 58.0 | 9.4 |
| 8 | Indus | -82.8 | -3.8 | -4.2 | 9.1 | -74.7 | 5.6 | 15.1 | -4.6 |
| 9 | Kolyma | -67.0 | -3.7 | -13.3 | 16.0 | -45.6 | 6.1 | 31.2 | -17.0 |
| 10 | Lena | 94.7 | 3.8 | 0.7 | 0.8 | 85.3 | -10.6 | -0.7 | 3.5 |
| 11 | Mackenzie | -54.1 | -6.2 | 16.5 | 23.3 | -20.1 | 10.7 | 64.3 | -4.8 |
| 12 | Mississippi | -36.8 | -0.2 | -20.4 | 42.7 | -17.4 | 0.2 | 51.5 | -30.9 |
| 13 | Niger | 79.1 | -1.6 | 15.9 | 3.5 | 81.4 | 1.4 | 15.6 | 1.6 |
| 14 | Nile | 61.8 | -8.1 | -13.4 | 16.7 | 68.1 | 6.8 | -11.2 | 13.9 |
| 15 | Northern Dvina | -29.0 | -11.7 | -19.8 | 39.6 | -6.1 | 15.4 | 39.3 | -39.2 |
| 16 | Ob | 83.5 | -9.5 | -1.9 | 5.2 | 70.1 | 17.1 | 7.1 | -5.7 |
| 17 | Olenek | 82.5 | 2.9 | 6.2 | 8.4 | 54.2 | -7.5 | 34.0 | -4.3 |
| 18 | Parana | -25.0 | -29.2 | 24.7 | 21.1 | 2.2 | 38.1 | 27.0 | 32.7 |
| 19 | Pearl | 96.4 | 2.2 | 0.3 | 1.1 | 83.5 | -9.8 | 1.8 | 5.0 |
| 20 | Pechora | 76.6 | -0.9 | 8.4 | 14.1 | 30.7 | 2.7 | 52.3 | -14.3 |
| 21 | Senegal | 86.4 | -2.2 | 7.9 | 3.5 | 94.6 | 0.9 | 4.5 | 0.0 |
| 22 | Volga | -41.3 | -13.5 | 39.6 | -5.6 | -12.0 | 20.2 | 49.6 | 18.1 |
| 23 | Yangtze | -26.2 | -19.1 | -11.6 | 43.1 | -4.6 | 24.6 | -19.8 | 51.0 |
| 24 | Yellow | -10.9 | -22.1 | -18.6 | 48.4 | -6.4 | 23.2 | -20.8 | 49.6 |
| 25 | Yenisei | 60.7 | -10.0 | -8.7 | 20.6 | 42.2 | 14.7 | -11.4 | 31.7 |
| 26 | Yukon | -63.8 | -1.3 | 19.6 | 15.3 | -25.7 | 2.6 | -20.8 | 50.9 |

Please also clearly state how to calculate the partial derivatives. Because these partial derivatives and the changes in the variables. Noting that the partial derivatives may change greatly (also see Zhou et al. (2016)), and will have large impacts on the results. The same issues also exist for the equations (11).

**Re: Yes, the partial derivatives are calculated by using the total differential method. We have added this before equation (10) and (11).**

Equation (11): use ≈ instead of = because SAI and M cannot fully explain the variation of the parameter n.

**Re: Yes, it has been done.**

Line 282: have a significant impact

**Re: Yes, we have revised it.**

Line 297: b is negative while c is positive

**Re: Yes, we have revised it. Thank you!**

Equation (14): please calibrate the parameter a, b, c in each catchment (add a table or figure for this), and show whether the parameters are robust across different regions.

**Re: Thank you for your kind suggestion. We have added a table to summary these parameters and its robustness for each catchment (Table S1 in Supplement). In addition, we also added more analysis for this Table. The text states as follow:**

**"In addition, the Eq. (13) has also been verified in each catchment among the 26 basins (Table S1). The RMSE and MAE for each catchment is relatively small with mean values of 12.0 and 14.8 mm, respectively. Except for basins 3, 5 and 26, the $R^2$ values for simulation of *R* in each catchment are larger than 0.5. These results indicated that the M and SAI as well as the semi-empirical formula can well explain the variability of the controlling parameter *n*."**

**Table S1.** The validated parameter of eq. (14) and simulation accuracy of *R* based on the estimated *n* with the validated parameters for each basin

| ID | Validated basin | Model coefficients | | | *R* simulation accuracy | | |
|---|---|---|---|---|---|---|---|
| | | *a* | *b* | *c* | $R^2$ | RMSE | MAE |
| 1 | Amur | 5.05 | -0.36 | -0.05 | 0.90 | 32.7 | 26.4 |
| 2 | Aral | $0.39^{*}$ | $0.77^{*}$ | 0.04 | 0.80 | 7.9 | 6.1 |
| 3 | Columbia | $0.58^{***}$ | 0.47 | -0.06 | 0.27 | 12.2 | 9.9 |
| 4 | Congo | 0.92 | 0.10 | $-0.36^{***}$ | 0.94 | 12.8 | 10.7 |
| 5 | Danube | 0.42 | 0.81 | -0.21 | 0.22 | 39.4 | 35.4 |
| 6 | Indigirka | 0.02 | $2.37^{***}$ | -0.02 | 0.85 | 16.1 | 13.1 |
| 7 | Indus | $0.26^{*}$ | 0.57 | $0.59^{*}$ | 0.82 | 11.6 | 9.3 |
| 8 | Kolyma | $0.34^{*}$ | $0.98^{**}$ | -0.20 | 0.60 | 19.2 | 16.5 |
| 9 | Lena | $0.39^{***}$ | $0.71^{**}$ | 0.19 | 0.84 | 9.0 | 7.1 |
| 10 | Mackenzie | $0.28^{*}$ | $0.91^{**}$ | -0.04 | 0.95 | 6.3 | 5.2 |
| 11 | Mississippi | $1.06^{*}$ | -0.03 | 0.00 | 0.81 | 8.9 | 6.9 |
| 12 | Niger | 0.03 | $2.22^{*}$ | 0.03 | 0.63 | 24.3 | 18.3 |
| 13 | Nile | $0.99^{***}$ | -0.17 | 0.06 | 0.80 | 14.1 | 10.4 |
| 14 | Northern Dvina | $1.53^{*}$ | -0.33 | -0.01 | 0.64 | 10.8 | 8.9 |
| 15 | Ob | 0.34 | 0.61 | $0.30^{**}$ | 0.85 | 14.3 | 11.5 |
| 16 | Olenek | 0.33 | $0.76^{*}$ | 0.10 | 0.82 | 10.3 | 8.4 |
| 17 | Parana | $0.35^{***}$ | $0.60^{*}$ | 0.39 | 0.76 | 11.4 | 8.3 |
| 18 | Pearl | 2.90 | -0.10 | $-0.16^{**}$ | 0.80 | 15.7 | 12.9 |
| 19 | Pechora | 0.09 | $1.40^{*}$ | -0.01 | 0.97 | 21.8 | 17.2 |
| 20 | Senegal | 0.44 | 0.44 | 0.06 | 0.87 | 16.5 | 13.1 |
| 21 | Volga | $1.48^{***}$ | -0.04 | $-0.41^{*}$ | 0.82 | 4.0 | 3.3 |
| 22 | Yangtze | 0.29 | 0.87 | -0.02 | 0.76 | 13.4 | 10.3 |
| 23 | Yellow | 0.45 | 0.30 | -0.06 | 0.92 | 19.3 | 15.6 |
| 24 | Yenisei | 0.86 | 0.28 | -0.01 | 0.58 | 11.0 | 9.1 |

| | | | | | | | |
|---|---|---|---|---|---|---|---|
| 25 | Yukon | 0.32 | 0.79* | 0.02 | 0.80 | 6.0 | 4.7 |
| 26 | Amur | 0.13 | 1.06 | 0.12 | 0.43 | 16.4 | 14.4 |
| | All basins | 0.29*** | 0.86*** | -3.3*** | 0.92 | 68.2 | 45.8 |

'*', '**' and '***' represent the validated parameter are significant at the level of $p$ = 0.1, $p$ = 0.05 and $p$ = 0.01, respectively.

Line 303: You should check the relationship between SAI and M before the calibration. If SAI and M are correlated, you should not use multiple linear regression because of multicollinearity problems. Please use partial least square regression to calibrate the parameters.

**Re: Thank you for your kind comments. We have used the partial least square regression (PLSR) to replace the multiple linear regression (MLR). It is worth mentioning that MLR (or PLSR) in this study is used as a comparison to analysis the performance of the semi-empirical formula (SEF). And the results show that the SEF performance much better than the MLR and PLSR. Therefore, the replacement of MLR has no effect on the later calculations and final results.**

Line 303 and other sentences: change formulae to formula

**Re: Yes, it has been done.**

Lines 301-304: please show the calibrated parameters for the cross-validation, at least in the supporting information.

**Re: Thank you for your kind comments. The calibrated parameters for cross validation has been added in the revised manuscript (Table 2 in supplement).**

**Table S2.** The validated parameter for the cross-variation of $n$.

| ID | Validated basin | $a$ | $b$ | $c$ | ID | Validated basin | $a$ | $b$ | $c$ |
|---|---|---|---|---|---|---|---|---|---|
| 1 | Amur | 0.28*** | 0.88*** | -0.32*** | 14 | Northern Dvina | 0.29*** | 0.86*** | -0.33*** |
| 2 | Aral | 0.28*** | 0.87*** | -0.33*** | 15 | Ob | 0.28*** | 0.90*** | -0.29*** |
| 3 | Columbia | 0.27*** | 0.90*** | -0.31*** | 16 | Olenek | 0.29*** | 0.86*** | -0.33*** |
| 4 | Congo | 0.29*** | 0.86*** | -0.32*** | 17 | Parana | 0.28*** | 0.87*** | -0.33*** |
| 5 | Danube | 0.29*** | 0.88*** | -0.13*** | 18 | Pearl | 0.32*** | 0.77*** | -0.36*** |
| 6 | Indigirka | 0.29*** | 0.85*** | -0.33*** | 19 | Pechora | 0.29*** | 0.87*** | -0.32*** |
| 7 | Indus | 0.29*** | 0.86*** | -0.33*** | 20 | Senegal | 0.30*** | 0.83*** | -0.33*** |
| 8 | Kolyma | 0.27*** | 0.88*** | -0.32*** | 21 | Volga | 0.26*** | 0.91*** | -0.33*** |
| 9 | Lena | 0.28*** | 0.88*** | -0.32*** | 22 | Yangtze | 0.29*** | 0.85*** | -0.34*** |
| 10 | Mackenzie | 0.29*** | 0.86*** | -0.33*** | 23 | Yellow | 0.34*** | 0.76*** | -0.39*** |
| 11 | Mississippi | 0.29*** | 0.86*** | -0.33*** | 24 | Yenisei | 0.26*** | 0.90*** | -0.32*** |
| 12 | Niger | 0.29*** | 0.86*** | -0.33*** | 25 | Yukon | 0.29*** | 0.85*** | -0.33*** |
| 13 | Nile | 0.28*** | 0.87*** | -0.33*** | 26 | Amur | 0.30*** | 0.83*** | -0.32*** |

'***' represent the validated parameter are significant at the level of $p$ = 0.01

Lines 315-320: also plot the relationships between the simulated R and E using the equation (14) and the observed values.

**Re: Thank you for your kind comments. The subgraphs for simulated *R* and *E* using the equation (14) has been added in Figure 7. More analyses have been added in the revised manuscript. The text states as follow.**

"As shown in Fig. 7a-b, the simulated annual *R* and *E* that estimated by Budyko model with cross-validation parameter *n* showed a remarkable agreement with the observed ones with *NSE* larger than 0.89 and MAE smaller than 50.52 mm, which is close to the simulation accuracy of these estimated by Budyko model with simulated parameter *n* by using the semi-empirical formula (i.e., eq. (14) (Fig. 7c-d)."

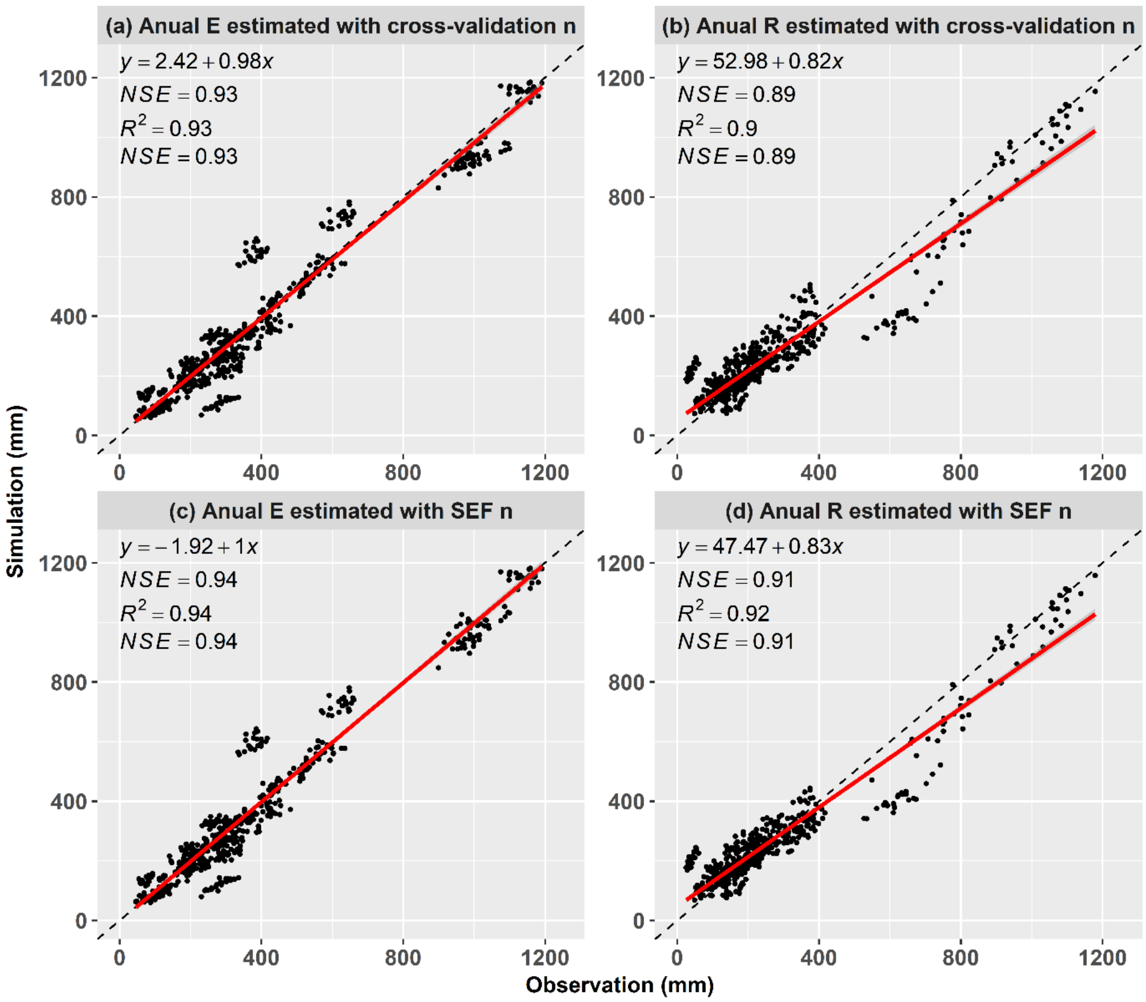


**Figure 7.** The observed *E* and *R* versus the simulated *E* and *R* estimated by Budyko model with simulated parameter *n* by (a-b) eq. (13) with cross-validation method and (c-d) eq. (14)

Lines 342-343: because of the monsoon variability, see Cook et al. (2010).

Cook, E. R., Anchukaitis, K. J., Buckley, B. M., D'Arrigo, R. D., Jacoby, G. C., & Wright, W. E. (2010). Asian monsoon failure and megadrought during the last millennium. Science, 328(5977), 486-489.

**Re: Thank you for your kind suggestion. It has been added.**

Lines 376-384: **(a)** The equations (13) and (14) are used to mainly explain temporal variations of the parameter n, and may not be useful to explain the spatial variations, especailly when large variations in land surface characteristics exist. **(b)** Are the remaining scatters in figure 4 related to different land surface characteristics? **(c)** I am wondering whether the explanatory power of the equation (13) is larger when it is applied to each one basin, than for all basins.

**Re: Thanks so much for your kind comments. To test the performance of the semi-empirical formula in the modelling of spatial variations of parameter *n*, we also recalibrated the equation (13) at the long-term time scale. Then we obtained a semi-empirical formula for spatial variations of parameter *n*: $n = 0.33\mathrm{SAI}^{-0.39}\mathrm{M}^{0.77}$, the regression coefficient of which is closed to the equations (14). As shown in below Figure S1, the spatial variation of *n* simulated by this formula match well with the optimized *n* with *NSE* of 0.8 and *MAE* of 0.2. In addition, the simulated long-term *R* and *E* that estimated by Budyko model with simulated long-term *n* showed a remarkable agreement with the observed ones with $R^2$ larger than 0.91 and MAE smaller than 40 mm (Figure S2), which is also similar to the simulation accuracy of these estimated by Budyko model with simulated parameter *n* by eq. (14) at annual time scale (Figure 7b-c). These results suggest that the semi-empirical formula is also useful to explain the spatial variations of parameter *n*.**

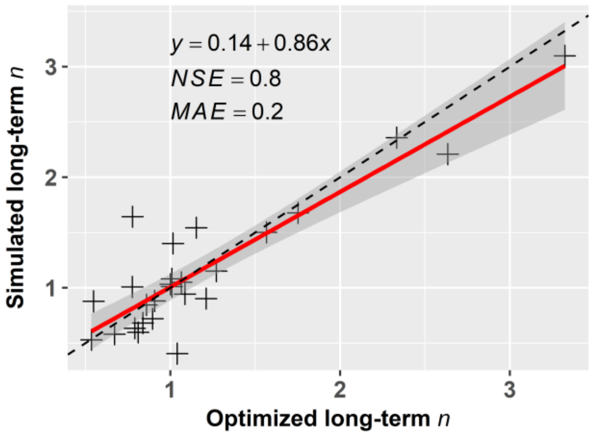


**Figure S1.** The Optimized long-term *n* versus the versus simulated long-term *n* estimated by eq. (13).

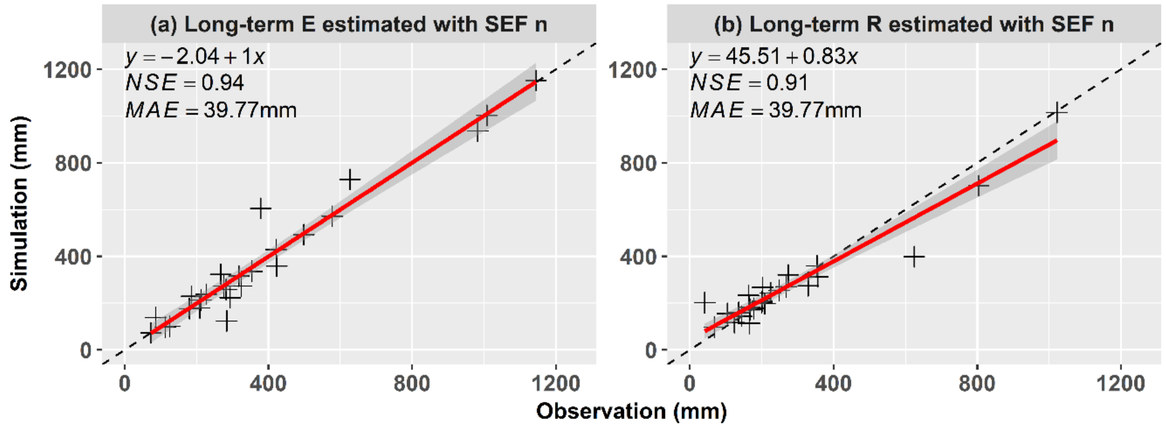


**Figure S2.** The observed long-term *E* and *R* versus the versus simulated long-term *E* and *R* estimated by Budyko model with simulated parameter *n* by eq. (13).

**(b) Yes, you are right. The remaining scatters all belongs to the Congo river basin, which located at tropical areas. Besides, the Congo river is the deepest river across the world with steep gradients and large flow velocity. Therefore, The Congo river basin represented by the remaining scatters has different land surface characteristics compared with other basins. If we deleted the scatter of Congo, the remaining scatters in figure 4 disappear (Shown as below figure).**

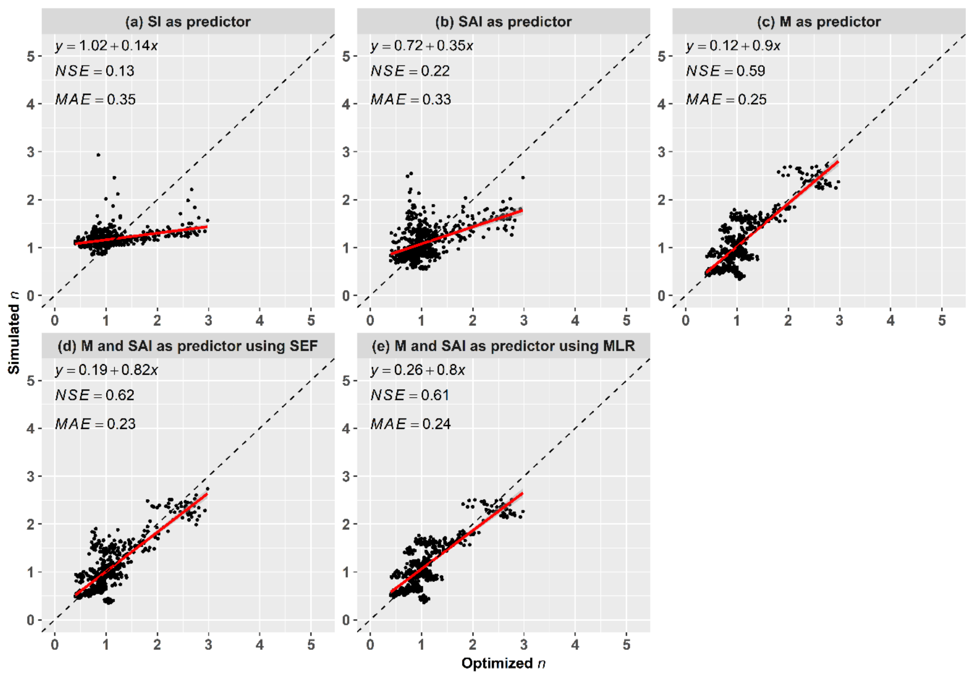


**Figure S3.** Same to Figure 4 but excluded the Congo river basin.

**(c) Yes, the explanatory power of the equation (13) is larger when it is applied to each one basin, than for all basins. As shown in the Table S1 in Supplement, the RMSE and MAE of simulated runoff based on the *n* estimated by each one basin is obvious smaller than these for all basins, with the mean value of 16.8, 13.3mm; However, the $R^2$ of simulated runoff calculated by equation (14) for all basins is large than simulated runoff combined by each basin and calculated by equation (13).**

Lines 396-400: why other factors such as precipitation contribute a small proporation to R and E in the Danube river basin. Please change river to river basin here and other places.

**Re: We have added a table to show the detailed the change of P, R, E as well as other factors (Table S3 in Supplement). As shown in Table S3, the absolute rate of change in precipitation is much smaller than *R* and *E*, with 5.2% for the former but 12.9% and 16.3% for the later. What's more, the change direction of *R* is different to the *P*. These indicate that the *R* and *E* changes in Danube river basin is dominant by other factors, rather than precipitation. By the way, the river has been revised to river basin in the full-text. Thank you.**

**Table S3.** The change points of runoff and the change rates of meteorological and vegetative factors after change points

| ID | Basin | Changepoint of *R* | *R* | *E* | *Pe* | *PET* | *n* | *NDVI* | *SI* |
|---|---|---|---|---|---|---|---|---|---|
| 1 | Amazon | 1998 | 8.5 | -1.0 | 3.4 | 1.1 | -9.4 | 3.4 | 0.3 |
| 2 | Amur | 1998 | -16.4 | -0.3 | -5.8 | 3.0 | 4.5 | -1.3 | 24.9 |
| 3 | Aral | 1994 | -14.8 | 12.8 | 5.2 | 3.8 | 12.4 | -0.8 | -6.1 |
| 4 | Columbia | 1999 | -10.7 | 1.2 | -4.4 | 4.2 | 2.1 | -1.7 | 15.7 |
| 5 | Congo | 1997 | 4.1 | -2.5 | -0.8 | 0.7 | -15.5 | 1.0 | 3.5 |
| 6 | Danube | 1988 | -12.5 | 16.4 | 5.2 | 5.5 | 27.3 | 6.4 | 1.4 |
| 7 | Indigirka | 1990 | -7.0 | 4.4 | -3.4 | 2.4 | 5.0 | 5.5 | 5.1 |
| 8 | Indus | 1998 | -16.7 | -4.5 | -9.0 | 1.7 | 2.3 | 3.4 | 24.6 |
| 9 | Kolyma | 1990 | -9.6 | 0.4 | -5.0 | 0.9 | 3.7 | 4.2 | 16.9 |
| 10 | Lena | 1995 | 14.3 | 4.7 | 9.2 | -1.3 | 0.3 | 1.1 | -3.8 |
| 11 | Mackenzie | 1989 | -13.3 | 6.2 | -3.5 | 2.3 | 10.5 | -2.7 | 13.1 |
| 12 | Mississippi | 1998 | -20.1 | 5.0 | -2.0 | 0.0 | 15.1 | 1.3 | 8.7 |
| 13 | Niger | 1990 | 27.9 | 7.7 | 13.7 | 0.6 | -2.6 | 6.5 | -4.1 |
| 14 | Nile | 1995 | 14.7 | 3.2 | 5.7 | 1.9 | -2.9 | 3.1 | 12.5 |
| 15 | Northern Dvina | 2000 | -7.1 | 6.7 | -1.1 | 2.2 | 9.4 | 1.3 | 8.5 |
| 16 | Ob | 1998 | 7.5 | 4.7 | 5.9 | 1.8 | 0.9 | -0.8 | -7.0 |
| 17 | Olenek | 1988 | 13.9 | 10.7 | 12.6 | -1.9 | 4.5 | 6.2 | -20.5 |
| 18 | Parana | 1998 | -6.6 | 2.0 | 0.1 | 1.6 | 4.6 | -1.1 | 2.9 |

| | | | | | | | | | |
|---|---|---|---|---|---|---|---|---|---|
| 19 | Pearl | 1991 | 16.3 | 2.9 | 10.1 | -0.7 | -0.5 | -1.6 | 19.0 |
| 20 | Pechora | 1990 | 20.4 | -3.9 | 11.1 | 0.7 | -10.2 | 2.7 | -12.4 |
| 21 | Senegal | 1993 | 28.3 | 15.3 | 16.9 | 0.9 | 1.7 | 7.6 | -9.3 |
| 22 | Volga | 1994 | -8.9 | 4.1 | -1.2 | 2.3 | 6.8 | 3.8 | 1.6 |
| 23 | Yangtze | 2000 | -4.5 | 5.9 | -0.6 | 3.0 | 5.2 | -0.3 | -3.2 |
| 24 | Yellow | 1990 | -10.1 | 3.2 | -0.3 | 2.9 | 5.1 | 2.6 | 24.2 |
| 25 | Yenisei | 1996 | 2.1 | 3.9 | 3.1 | 1.1 | 2.3 | 1.6 | 12.1 |
| 26 | Yukon | 1994 | -8.0 | -28.4 | -15.6 | 2.2 | -18.9 | -3.4 | 8.9 |

Lines 401-402: n is only a parameter without specific physical meanings.

**Re: Yes, it has been modified as “**the impact of **other factors represented by parameter** *n* on the water balance not only includes SAI and M**…”**

------------------------------------ Reviewer #2 --------------------------------------

Understanding the effects and mechanisms of climate variability and vegetation dynamics on fluvial water balance is helpful for hydrological modeling, forecasting and water management. Several studies assessed the impacts of the mismatch in water and energy in terms of a seasonality index (SI) on hydrological cycle, such as Milly, 1994, Woods, 2003. However, previous studies didn't consider the phase difference between seasonal P and E0. Hence, the authors proposed a new index, named climate seasonality and asynchrony index (SAI). They found that the SAI performs much better than the old SI in Budyko framework. On this account, the authors make an important addition to the literature of hydrological studies. In general, the manuscript is in the scope of HESS and I agree with its scientific objective. Especially, the proposed SAI, and the semi-empirical formula for the spatiotemporal variation of parameter n are valuable for the Budyko framework related hydrological studies. Therefore, I strongly recommend acceptance of this paper in view of its importance and newness in results after minor revisions.

**Re: Thank you so much for your recognition to the article. We feel great appreciate for your professional review work on our manuscript. We will modify this paper strictly according to your request.**

1. Abstract: The first sentence of the abstract, what's the meaning of "The partitioning of water and energy"?

**Re: It means that the partitioning of precipitation between evapotranspiration and streamflow. This sentence has been rephrased as "The partitioning of precipitation into runoff (*R*) and evapotranspiration (*E*), governed by the controlling parameter in the Budyko framework (i.e., *n* parameter in the Choudhury and Yang equation), is critical to assess the water balance at global scale."**

2. Abstract: "a climate seasonality and asynchrony index (SAI) were proposed in terms of both phase and amplitude mismatch between P and E0." Who proposed SAI? Please rephrased this sentence.

**Re: We are sorry for our unclear statement. This sentence has been rephrased as follow:** "To reflect the mismatch between water supply (precipitation, $P$) and energy (potential evapotranspiration, $E_0$), **we proposed** a climate seasonality and asynchrony index (SAI) in terms of both phase and amplitude mismatch between $P$ and $E_0$."

3. Introduction: The authors should provide a nicer literature review, so they can have a clearer description of the novelty of this study. Their current lecture review is not sufficient to refer back to the literature. Berghuijs and Woods 2016 and Abatzoglou and Ficklin, 2018 have also considered climate seasonality into Budyko. The authors should state the differences between their work and existing studies.

**Re: As suggested by the reviewer, we have added more references to review the climate seasonality. The SAI proposed in this study is based on the hypothesis that the monthly precipitation and potential**

**evapotranspiration are follow the sine function. Fittingly, Berghuijs and Woods (2016) found that the sine function can fully describe the vast majority of the monthly precipitation and temperature over the globe. But they didn't investigate the climate seasonality, i.e., the mismatch of water and energy. However, this reference is important to support the SAI, we added this reference in the method.**

**Similar to previous studies (Woods, 2003; Ning et al., 2017; Yang et al., 2012), the climate seasonality used in Abatzoglou and Ficklin (2018) also have not considered the phase mismatch between *P* and $E_0$. We have added this reference in revised manuscript. The text states as follow: "Climate seasonality (SI) was identified to reflect the non-uniformity in the intra-annual distribution of water and energy, which plays a role in the variation of controlling parameter in the Budyko model (Woods, 2003; Ning et al., 2017; Yang et al., 2012; Abatzoglou and Ficklin, 2017). It is noted that distributions of water and energy were reflected not only by differences of seasonal amplitudes of *P* and $E_0$ but also by the phase mismatch between *P* and $E_0$. In this case, we proposed a climate seasonality and asynchrony index (SAI) to reflect the seasonality and asynchrony of water and energy distribution."**

4. Equation (11): The authors decomposed the changes of parameter n as a function of SAI and M. How does this work? Do they used complementary method? or Total differential decomposition? Please give more details. Either way, the authors should explain how they subdivided series into two periods.

**Re: The decomposition of n into SAI and M is based on the total differential method, which has been added in the revised manuscript. We subdivided the series into two periods based on the changepoint. We have added more details to explain how we do this in the revised manuscript. The text states as:**

**"**We used Ordered clustering test, Pettitt test method and AMOC method to detect the change points of *R*. To avoid possible uncertainty results based on the individual method, the assembled change points were confirmed with more than one method. If the results for all the three methods are different, the median change point would be selected (Liu et al., 2017a). Based on the changepoints of *R* and the changes rates of $P_e$, $E_0$, M and SAI before and after change points (Table S3 in the supplement), the contributions of these four factors to *R* and *E* were assessed (Figures 8 and 9; Table S3).**"**

5. Figure 3: the color for the below three subgraphs is difficult to distinguish. I suggest the authors used the larger plots and a discrete color bar with more different colors.

**Re: Thank you for your kind suggestion. We have remade these subgraphs (shown as below).**

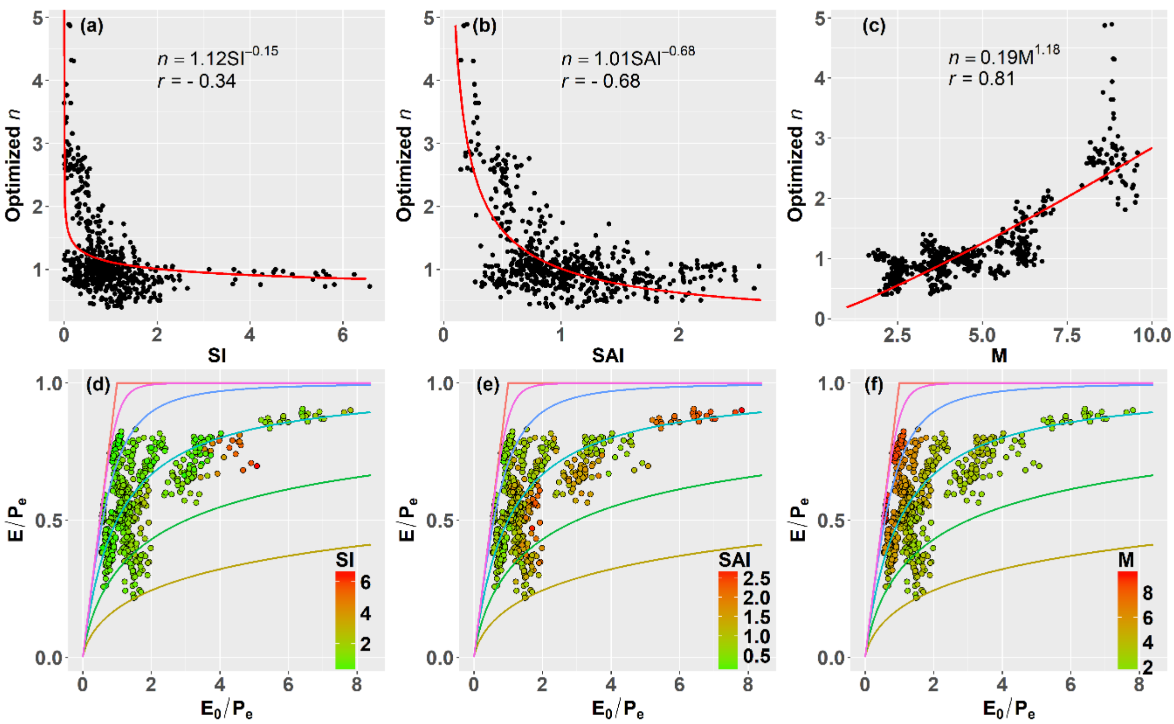


**Figure 4.** Relationship between optimized $n$ and (a) SI, (b) SAI and (c) M. (d-f) Distribution of evapotranspiration ratio ($E/P_e$) as a function of the aridity index ($E_0/P_e$) classified by 26 global large river basins at annual scale. The Budyko curves from the top down are derived from eq. (2b) with $n$=∞, $n$=5, $n$=2, $n$=1, $n$=0.6 and $n$=0.4, respectively. Noted that each point represents one year based on the combined dataset from 26 global large basins.

6. In figure 4 and 6, the author used the R2 and MAE to assess the simulation accuracy. I am curious that why they didn't use the Nash-Sutcliffe efficiency. A high R2 just means a high relationship, rather than a high accuracy.

**Re: Thank you for your kind suggestion. The R2 has been added in the Figure 5 and 7.**

7. The structure of 4.1 section is difficult to follow. They analysis the Figure 3 and 4 in the first paragraph, then they analyze the Figure 3 again in the next paragraph. Please recombine these sentences.

**Re: Thank you for your kind comment. We have recombined and rephrased this section to make it easy to follow. In the 4.1 section, we split the first paragraph into two parts, and then combined the latter part with the third paragraph as the second paragraph. Finally, we rephrased the fourth paragraph.**

8. The authors descript the mismatch of water and energy in three scenarios in terms of the SAI and 1-DI. However, does the SAI always belong to these scenarios? How about SAI = 1-DI or SAI = DI-1? Given that the SAI is the main innovation of this study, I suggest the authors give some illustrations for these scenarios of SAI.

**Re: We have merge the case of SAI = 1-DI or SAI = DI-1 into the third case, that is (3) SAI ≥ |DI − 1|, given that a larger SAI implies more surplus of *P* for the wet season with *P*(*t*) > $E_0$ (*t*).**

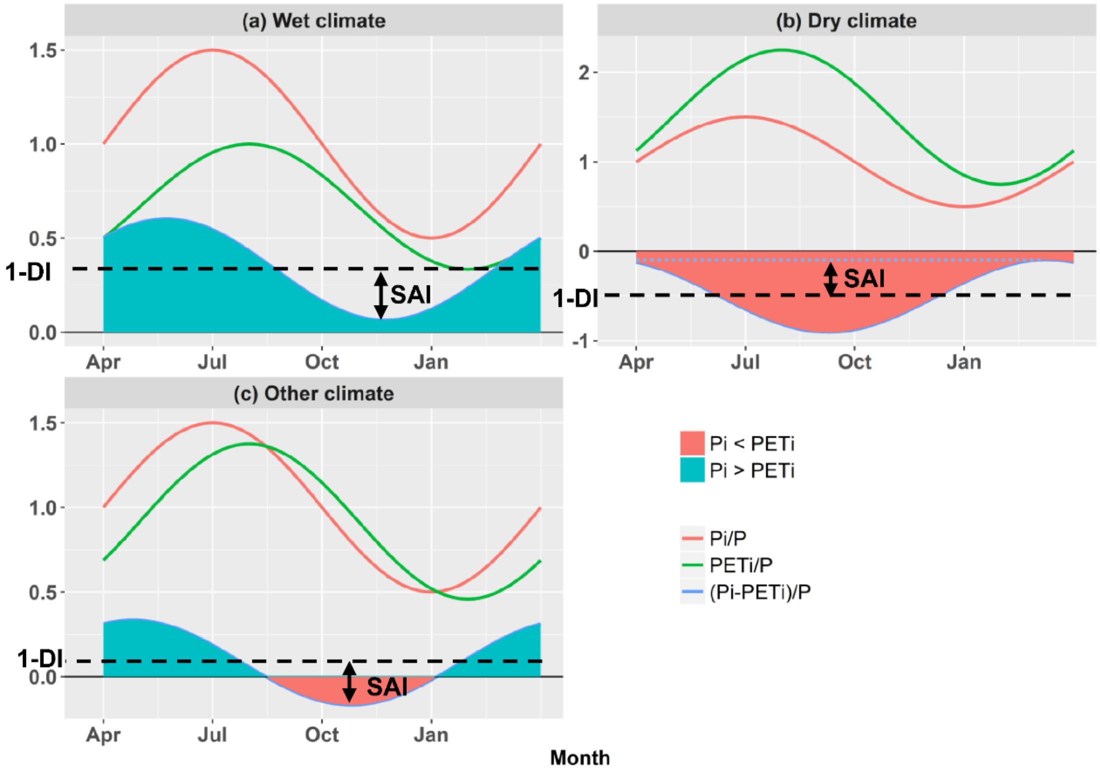


**Figure 3.** Examples of three scenarios for the mismatch between water and energy in terms of the relationship of SAI to 1-DI. (a) SAI smaller than 1-DI, implying *P* larger than PET in the whole year. (b) SAI smaller than DI-1, implying *P* small than PET in the whole year. (c) SAI smaller than 1-DI, implying a larger SAI means more surplus of *P*. The shaded areas represent the difference between precipitation and potential evapotranspiration, which equal to $(1 - DI) + \text{SAI}\sin\left(\frac{2\pi}{\tau}\frac{t}{12} + \varphi\right)$.

## 2. The list of all relevant changes made in the manuscript

(1) A Figure (Fig. 3) was added.

(2) Two subgraphs were added in Fig. 7.

(3) The NSE values were added in Figs. 6 and 8.

(4) Four tables were added in the supplement.

(5) Some values were corrected after a thorough examination, which have little effects on the results.

(6) More introduction about the Budyko function was added.

(7) The process for calculation of contribution was added.

(8) Xihui, Gu, who helps a lot in the modification of manuscript, was added in the authors.

# Hydrological effects of climate variability and vegetation dynamics on annual fluvial water balance at global large river basins

Jianyu Liu, Qiang Zhang*, Vijay P. Singh, Changqing Song, Yongqiang Zhang, Peng Sun, Xihui, Gu

**Corresponding author:**

Qiang Zhang, Ph.D. Professor, Associate editor of HSJ and JH

Key Laboratory of Environmental Changes and Natural Hazards, Ministry of Education, Academy of Hazard Reduction and Emergency Management, & State Key Laboratory of Earth Surface Processes and Resource Ecology

Beijing Normal University

Beijing 100875,

China.

Tel: +86-10-58807086

E-mail: zhangq68@bnu.edu.cn (preferred contact address)

**Hydrological effects of climate variability and vegetation dynamics on annual fluvial water balance at global large river basins**

Jianyu Liu[1], Qiang Zhang[2,3,4*], Vijay P. Singh[5], Changqing Song[2,3,4], Yongqiang Zhang[6], Peng Sun[7], Xihui, Gu[8]

[1]Laboratory of Critical Zone Evolution, School of Earth Sciences, China University of Geosciences, Wuhan 430074, China

[2]Key Laboratory of Environmental Change and Natural Disaster, Ministry of Education, Beijing Normal University, Beijing 100875, China

[3]State Key Laboratory of Earth Surface Processes and Resource Ecology, Beijing Normal University, Beijing 100875, China

[4]Faculty of Geographical Science, Academy of Disaster Reduction and Emergency Management, Beijing Normal University, Beijing 100875, China

[5]Department of Biological and Agricultural Engineering and Zachry Department of Civil Engineering, Texas A&M University, College Station, Texas, USA

[6]CSIRO Land and Water, GPO Box 1700, Canberra ACT 2601, Australia

[7]College of Geography and Tourism, Anhui Normal University, Anhui 241000, China

[8]Department of Atmospheric Science, School of Environmental Studies, China University of Geosciences, Wuhan 430074, China;

**Abstract:** The partitioning of precipitation into runoff ($R$) and evapotranspiration ($E$)~~water and energy~~, governed by the controlling parameter in the Budyko framework (i.e., $n$ parameter in the Choudhury and Yang equation), is critical to assess the water balance at global scale. It is widely acknowledged that the spatial variation of this controlling parameter is affected by landscape characteristics, but characterizing its temporal variation remains yet to be done. Considering effective precipitation ($P_e$), the Budyko framework was extended to the annual water balance analysis. To reflect the mismatch between water supply (precipitation, $P$) and energy (potential evapotranspiration, $E_0$), we proposed a climate seasonality and asynchrony index (SAI) ~~were~~ was ~~proposed~~ in terms of both phase and amplitude mismatch between $P$ and $E_0$. Considering streamflow changes in 26 large river basins as a case study, SAI was found to the key factor explaining ~~46~~51% of the annual variance of parameter $n$. Furthermore, the vegetation dynamics ($M$) remarkably impacted the temporal variation of $n$, explaining 67% of the variance. With SAI and M, a semi-empirical formula for parameter $n$ was developed at the annual scale to describe annual runoff ($R$) and evapotranspiration ($E$). The impacts of climate variability ($P_e$, $E_0$ and SAI) and M on $R$ and $E$ changes were then quantified. Results showed that $R$ and $E$ changes were controlled mainly by the $P_e$ variations in most river basins over the globe, while SAI acted as the controlling factor modifying $R$ and $E$ changes in the East Asian subtropical monsoon zone. SAI, M and $E_0$ have large impacts on $E$ than on $R$, whereas $P_e$ has larger impacts on $R$.~~, $E_0$ in the temperate maritime climate of Europe, and M in the temperate grassland zone of South America.~~

## 1. Introduction

Climate variability, vegetation dynamics and water balance are interactive, and this interaction is critical in the evaluation of the impact of climate change and vegetation dynamics on water balance at the basin scale and for the management of water resources (Milly, 1994; Yang et al., 2009; Weiss et al., 2014; Zhang et al., 2016c). The models that can quantify the climate-vegetation-hydrology interactions without calibration using observed evapotranspiration/runoff are particularly needed for hydrological prediction in ungauged basins (Potter et al., 2005). Furthermore, quantifying the influence of climate variability and vegetation dynamics on hydrological variability is critical in differentiating the factors that drive the hydrological cycle in both space and time (Yan et al., 2014; Dagon and Schrag, 2016; Zhang et al., 2016a).

The Budyko framework was developed to quantify the partitioning of precipitation into runoff and evapotranspiration (Koster and Suarez, 1999; Xu et al., 2013), and was widely used to evaluate interactions amongst climate, catchment characteristics, and hydrological cycle (Yang et al., 2009; Cai et al., 2014; Liu et al., 2017b; Ning et al., 2017). However, the controlling parameter of the Budyko framework usually needs to be calibrated, based on observed data. If the controlling parameter can be determined using the available data, then the Budyko framework can be employed in modelling the hydrological cycle in ungauged basins (Li et al., 2013). That is why considerable attention has been devoted to quantifying the relationship between the controlling parameter and explanatory variables (e.g. Yang et al., 2009; Abatzoglou and Ficklin, 2017). Most of the relationships were evaluated at a long-term scale (Abatzoglou and Ficklin, 2017; Gentine et al., 2012; Li et al., 2013; Xu et al., 2013; Yang et al., 2009; Yang et al., 2007; Zhang et al., 2016c) due to the steady-state assumption of the Budyko model. However, hydrological processes, such as water storage, are usually nonstationary due to climate change and human activities (Greve et al., 2015; Ye et al., 2015). It should be noted here that the variability of controlling parameters from year to year may be considerably large in a specific river basin, which can be significantly affected by variations in vegetation cover and climate conditions. Hence, it is necessary to develop a model to estimate annual variations of controlling parameters. In a recent study, Ning et al. (2017) established an empirical relationship of the controlling parameter at the annual scale in the Loess Plateau of China. However, the annual values of the optimized controlling parameter in their study were calibrated with the *Fu* equation without consideration of the annual water storage changes ($\Delta S$). But $\Delta S$ was identified as a key factor causing annual variations of water balance in most river basins, particularly in river basins of arid regions (e.g. Chen et al., 2013). Therefore, considering water storage changes, the effective precipitation ($P_e$), which is the difference between precipitation and water storage change (Chen et al., 2013), was used to extend the Budyko framework to annual-scale water balance analysis and was used to calibrate $n$.

Climate seasonality (SI) was identified to reflect the non-uniformity in the intra-annual distribution of water and energy, which plays a role in the variation of controlling parameter in the Budyko model (Woods, 2003; Ning et al., 2017; Yang et al., 2012; Abatzoglou and Ficklin, 2017). It is noted that distributions of water and energy were reflected not only by differences of seasonal amplitudes of $P$ and $E_0$ but also by the phase mismatch between $P$ and $E_0$. In this case, we proposed a climate seasonality and asynchrony index (SAI) to reflect the seasonality and asynchrony of water and energy distribution.

Vegetation coverage has also been found to be closely related to the spatial variation of the controlling parameter (Yang et al., 2009). Li et al. (2013) and Xu et al. (2013) used vegetation coverage to model the spatial variation of the controlling parameter in ~~26 river~~ the major large basins over the globe at a long-term scale. However, the effect of climate variability was not considered, and the impact of vegetation dynamics on the temporal variation of the controlling parameter was not fully investigated. Zhang et al. (2016c) established the relationship of parameter *n* with vegetation changes over northern China and suggested that the relationship needed to be further assessed in other river basins across the globe. Also, they confirmed the impact of climate seasonality on parameter *n*, and suggested future studies on its impacts on *n*. Therefore, this study devepoed a semi-empirical formula for parameter *n* with SAI and M as predictor variables at the annual scale, using meteorological and hydrological data from 26 large river basins from around the globe with a broad range of climate conditions.

Much work has been done, addressing water balance variations (e.g., Liu et al., 2017a; Zeng and Cai, 2016; Zhang et al., 2016a; Zhang et al., 2016b). For instance, Zeng and Cai (2016) evaluated the impacts of $P$, $E_0$ and ΔS on the temporal variation of evaportranspiration for large river basins. However, little is known about the influence of M and SAI on the hydrological cycle, particularly on their contributions to variations of runoff and evapotranspiration. The impact of M and SAI on the water balance is critical for water balance modelling. Therefore, based on the developed semi-empirical formula, this study further assessed the causes of variation of *R* and *E*. ~~Therefore, t~~The objectives of this study were: (1) to propose a climate seasonality and asynchrony index, SAI, to reflect the mismatch of water and energy; (2) to develop an empirical model for the controlling parameter *n* at the annual scale using data from

26 large river basins from around the globe; and (3) to investigate the impact of SAI and other factors on the *R* and *E* variations.

## 2. Data

Monthly terrestrial water budget data covering a period of 1984-2006 was collected from 32 large river basins from around the globe (Pan et al., 2012). The data set, including *P*, *E*, *R* and $\Delta S$, combined data from multiple sources, such as in situ observations, remote sensing retrievals, model simulations, and global reanalysis products, which ~~was~~ were obtained using assimilation weighted with the estimated error. For more details on this dataset, reference can be made to Pan et al. (2012). This dataset, which was deemed to one of the best water budget estimates, has already been applied to assess the impact of vegetation, topography, latitude, and terrestrial storage on the spatial variability of the controlling parameter in the Budyko framework and the evapotranspiration variability over the past several years (Arnell and Gosling, 2013; Li et al., 2013; Xu et al., 2013; Zeng and Cai, 2016). The dataset has been designed to explicitly close the water budget. And that the use of data assimilation might lead to unphysical variability. As a result, Li et al. (2013) found that more than 20% of data in six basins among the 32 global basins were beyond the energy and water limits, and suggested analysis on water-energy balance using the remaining 26 basins. Following Li et al. (2013), we evaluated the impact of climate variability and vegetation dynamics on the spatiotemporal variation of the controlling parameter and the water balance of the 26 river basins. Detailed information about the characteristics of the 26 basins is given in Table 1. Monthly potential evapotranspiration ($E_0$) data from 1901 to 2015 at a spatial resolution of 0.5° was obtained from Climatic Research Unit of University of East Anglia (https://crudata.uea.ac.uk/cru/data/hrg/cru_ts_3.24.01/

cruts.1701201703.v3.24.01/pet/). Monthly normalized difference vegetation index (NDVI) covering a period of 1981-2006 was obtained from Global Inventory Modeling and Mapping Studies (GIMMS) (Buermann, 2002; Li et al., 2013).

## 3. Methods

### 3.1 The Budyko framework at annual scale

The Budyko framework has been widely used ~~to~~in assessment of ~~the~~ impacts of climate and vegetation variations on hydrological cycle. There are several analytical equations proposed under the Budyko framework, among which the function deduced by Choudhury (1999) and Yang et al. (2008) has been identified to perform better than other equations (Zhou et al., 2015). The ~~formula~~function can be expressed as:~~Based on the Budyko framework, Choudhury (1999) and Yang et al. (2008) deduced a water-energy formula as:~~

$$E = \frac{PE_0}{(P^n + E_0^n)^{1/n}} \qquad (1)$$

where $n$ is the controlling parameter of the Choudhury-Yang equation~~ which is one of the formulations of the Budyko framework~~.

The basin stores precipitation first and then releases it as runoff and evapotranspiration (Biswal, 2016). Affected by water storage changes, $E$ is always not equal to the difference between $P$ and $R$ for a short time interval. Previous studies have found that storage changes have impacts on water balance at the annual scale (Donohue et al., 2012). To consider the influence of variation of water storage, Wang (2012) suggested to use effective precipitation ($P_e$), i.e., $P_e = P - \Delta S$, to replace precipitation in the water-energy balance. As a result, using the $P_e$, the Choudhury and Yang equation (1999) can be extended in short time scale:

$$R = P_e - \frac{P_e E_0}{(P_e{}^n + E_0^n)^{1/n}} \tag{2a}$$

$$E = \frac{P_e E_0}{(P_e{}^n + E_0^n)^{1/n}} \tag{2b}$$

Parameter $n$ controls the shape of the Budyko curve and can be calibrated by minimizing the mean absolute error ($MAE$) of runoff (Legates and McCabe, 1999; Yang et al., 2007). Parameter $n$ is a catchment characteristic parameter which is mainly related to the underlying conditions (i.e., topography and soil), climate conditions, and vegetation cover (Liu et al., 2017a; Yang et al., 2009; Zhang et al., 2016c). The underlying characteristics are relatively stable during a short time interval, while climate and vegetation might undergo considerable variations, which can lead to the change of parameter $n$. As a result, vegetation dynamics and climate variability were applied to simulate $n$ and assess their impact on runoff and evapotranspiration.

The vegetation coverage ($M$), which is the fraction of land surface covered with green vegetation in the region, can be calculated as (Gutman and Ignatov, 1998):

$$M = (NDVI - NDVI_{min})/(NDVI_{max} - NDVI_{min}) \tag{3}$$

where $NDVI_{max}$ and $NDVI_{min}$ represent the dense green vegetation and bare soil with $NDVI_{max} = 0.80$ and $NDVI_{min} = 0.05$, respectively (Li et al., 2013; Ning et al., 2017; Yang et al., 2009).

### 3.2 Seasonality and asynchrony of water and energy

The seasonality of $P$ and $E_0$, which are mainly controlled by solar radiation, follows a sine distribution (Milly, 1994; Woods, 2003; Berghuijs and Woods (2016)):

$$P(t) = \bar{P}\left(1 + \delta_P \sin\left(\frac{2\pi}{\tau}\frac{t}{12}\right)\right) \tag{4a}$$

$$E_0(t) = \overline{E_0}\left(1 + \delta_{E_0} \sin\left(\frac{2\pi}{\tau}\frac{t}{12}\right)\right) \tag{4b}$$

where $t$ is the time (months), $P(t)$ and $E_0$ $(t)$ are the monthly $P$ and $E_0$ with the annual mean value of $\bar{P}$ and of $\overline{E_0}$, respectively. The quantities $\delta_P$ and $\delta_{E_0}$ are dimensionless seasonal amplitudes, which can be calibrated by minimizing *MAE*. The quantity $\tau$ is the cycle of seasonality, with half a year in the tropics and one year outside the tropics. The origin of time ($t = 0$) was fixed in April in the previous studies (Milly, 1994; Woods, 2003; Ning et al., 2017). As a result, if the $\delta_P$ ($\delta_{E_0}$) was positive, the month with maximum monthly $P$ ($E_0$) would appear in July, which corresponds to Northern Hemisphere (e.g., Figure 1a); while the southern Hemisphere would show a January maximum with negative $\delta_P$ ( $\delta_{E_0}$ ). Considering the difference between seasonal $P$ and $E_0$, Wood et al. (2003) defined a climate seasonality index by combining Eq. (4):

$$\mathrm{SI} = |\delta_P - \delta_{E_0} DI| \tag{5}$$

where *DI* is the dryness index ($\frac{\overline{E_0}}{\bar{P}}$).

<Figure 1 here please>

Equations (4) - (5) were applied to represent the mismatch between water and energy (e.g., Ning et al., 2017). However, the following two issues still need to be considered: (1) effect of local climate and catchment characteristics, the phase of seasonal $P$ and $E_0$ may be not entirely consistent with that of solar radiation; and (2) the phases between seasonal $P$ and $E_0$ cannot always be consistent in a specific basin, such as the Northern Dvina basin (Figure 1b). The values of $E$ for two basins with the same annual mean $P$, $E_0$, $\delta_P$ and $\delta_{E_0}$ can be different if the phases of seasonal $P$ and $E_0$ are in mismatch. As a result, the phase shifts of $P$ ($S_P$) and $E_0$ ($S_{E_0}$) should be considered in the sine function (Berghuijs and Woods, 2016):

$$P(t) = \bar{P}\left(1 + \delta_P \sin\left(\frac{2\pi}{\tau}\frac{t - S_P}{12}\right)\right) \tag{6a}$$

$$E_0(t) = \overline{E_0}\left(1 + \delta_{E_0} \sin\left(\frac{2\pi}{\tau}\frac{t - S_{E_0}}{12}\right)\right) \tag{6b}$$

As shown in figure 2, Eq. (6) with fitted phase performed much better in simulating monthly $P$ and $E_0$ than ~~eq.~~Eq. (4) with a fixed phase, with $R^2$ larger than 0.89 for the former but smaller than 0.64 for the latter.

<Figure 2 here please>

To fully reflect the difference between water and energy, it is necessary to consider not only the seasonal amplitude difference between $P$ and $E_0$, but also the phase difference (i.e., asynchrony) between them (Fig S1b). Therefore, an improved climate index describing the difference between water and energy needs to be developed with the consideration of seasonality and asynchrony of $P$ and $E_0$. Based on ~~eq.~~Eq. (6), we further deduced the following equations to express the difference between $P$ and $E_0$:

$$\frac{P(t)-E_0(t)}{\bar{P}} = (1-DI) + \left(\delta_P \sin\left(\frac{2\pi}{\tau}\frac{t-S_P}{12}\right) - DI\,\delta_{E_0}\sin\left(\frac{2\pi}{\tau}\frac{t-S_{E_0}}{12}\right)\right)$$

$$= (1-DI) + (a^2+b^2)^{1/2}\sin\left(\frac{2\pi}{\tau}\frac{t}{12}\cancel{-}+\varphi\right) \quad (7)$$

where $a = \delta_P \cos\frac{2\pi}{\tau}\frac{S_P}{12}\cancel{\delta_P} - DI\delta_{E_0}\cos\frac{2\pi}{\tau}\frac{S_{E_0}}{12}\cancel{\frac{S_P}{12}}$ , $b = -\delta_P \sin\frac{2\pi}{\tau}\frac{S_P}{12}\cancel{\delta_P} + DI\delta_{E_0}\sin\frac{2\pi}{\tau}\frac{S_{E_0}}{12}$ , $\varphi = \arctan(b/a)$. Similar to *Milly* (1994), we defined a seasonality and asynchrony index (SAI) to reflect the mismatch between water and energy in terms of the magnitude and phase difference between $P$ and $E_0$:

$$\mathrm{SAI} = (a^2+b^2)^{1/2}$$

$$= \left({\delta_P}^2 - 2\delta_P\delta_{E_0}DI\cos\left(\frac{2\pi}{\tau}\frac{S_P-S_{E_0}}{12}\right) + \left(\delta_{E_0}DI\right)^2\right)^{1/2} \quad (8)$$

The SI value calculated by ~~eq.~~Eq. (5) was an exceptional case for $P$ and $E_0$ in the same phase shifts. A larger SAI implies a greater difference between $P$ and $E_0$ in the year. Besides, SAI followed the following three scenarios: (1) $\mathrm{SAI} < 1-\mathrm{DI}$, given a wet climate with $P(t) > E_0(t)$ across the whole seasonal cycle (Fig. 3a); (2) $\mathrm{SAI} < \mathrm{DI}-1$, given a dry climate with $P(t)$

< $E_0$ ($t$) across the whole seasonal cycle (Fig. 3b); (3) SAI ≥~~>|~~DI − 1|, given that a larger SAI implies more surplus of $P$ for the wet season with $P(t) > E_0$ ($t$) (Fig. 3c).

### 3.3 Contributions of SAI and other factors to R and E

From ~~eq.~~Eq. (2), using total differential method, we can redefine the total differential of $R$ and $E$ for any time scale by introducing effective precipitation ($P_e$):

$$\mathrm{d}R \approx \frac{\partial R}{\partial P_e}\mathrm{d}P_e + \frac{\partial R}{\partial E_0}\mathrm{d}E_0 + \frac{\partial R}{\partial n}\mathrm{d}n \tag{9a}$$

$$\mathrm{d}E \approx \frac{\partial E}{\partial P_e}\mathrm{d}P_e + \frac{\partial E}{\partial E_0}\mathrm{d}E_0 + \frac{\partial E}{\partial n}\mathrm{d}n \tag{9b}$$

The climatic elasticity of evapotranspiration changes to the changes of precipitation, potential evapotranspiration and $n$ can be separately be expressed d as $\varepsilon_{P_e} = \frac{P_e}{E}\frac{\partial f}{\partial P_e}$ , $\varepsilon_{E_0} = \frac{E_0}{E}\frac{\partial f}{\partial E_0}$, $\varepsilon_n = \frac{n}{E}\frac{\partial f}{\partial n}$. The climatic elasticity of runoff changes is similar to the climatic elasticity evapotranspiration changes. The difference operator (d) in ~~eq.~~Eq. (9a) and ~~eq.~~Eq. (9b) refer to the difference of a variable before and after change points of $R$ and $E$, respectively. It is worth noting that ~~equations~~Eq. (9) ~~are~~is derived by the first-order approximation of Taylor expansion. When the changes of $\mathrm{d}P_e$, $\mathrm{d}E_0$ and $\mathrm{d}n$ are small, the error from approximation can be ignored. However, due to ignoring the higher orders of the Taylor expansion, the error will increase as the changes increase (Yang et al., 2014; Zhou et al., 20146; Yang et al., 2016).

The relative contribution (C) of $P_e, E_0$ and $n$ to the $R$ and $E$ changes can be obtained as:

$$C_{P_e} = \frac{I_{P_e}}{|I_P| + |I_{E_0}| + |I_n|},\quad C_{E_0} = \frac{I_{E_0}}{|I_P| + |I_{E_0}| + |I_n|},\quad C_n = \frac{I_n}{|I_P| + |I_{E_0}| + |I_n|} \tag{10}$$

$I_{P_e}, I_{E_0}$ and $I_n$ denote, respectively, the impacts of $P_e, E_0$ and $n$ on $R$ or $E$, which can be expressed by $\frac{\partial E}{\partial P_e}\mathrm{d}P_e$, $\frac{\partial E}{\partial E_0}\mathrm{d}E_0$ and $\frac{\partial E}{\partial n}\mathrm{d}n$, respectively. After getting the contribution of $n$ to the $R$ and $E$ variations, we can further assess the impacts of M and SAI on the variation of $R$ and $E$, based on the semi-empirical model of $n$ in terms of M and SAI. Following Ning et al. (2017), using the total differential method, the changes of parameter *n* can be expressed as follows:

$$dn \approx \frac{\partial n}{\partial \mathrm{SAI}}\mathrm{dSAI} + \frac{\partial n}{\partial \mathrm{M}}\mathrm{dM} \quad (11)$$

Then, the relative contributions of SAI ($C$_SAI) and M ($C$_M) to the changes of parameter *n* can be obtained. Combining with the contribution of *n* to the *R* and *E* changes, the relative contributions of SAI and M to the variations of *R* and *E* can be obtained:

$$C_{\mathrm{SAI}} = C_n \times \mathrm{C\_SAI}, \quad C_{\mathrm{M}} = C_{\mathrm{n}} \times C\_\mathrm{M} \quad (12)$$

## 4. Results

### 4.1 Performance of the proposed SAI in the Budyko framework

Figure 2 shows that ~~eq.~~Eq. (6) with SAI has a better performance in simulating *P* and $E_0$ than ~~eq.~~Eq. (4) with SI. Here we further assessed the performance of these two indices, by comparing with the controlling parameter *n* in the Budyko framework. Parameter *n* for each year was first calibrated by ~~eq.~~Eq. (2). The calibrated parameter *n* was called optimized *n*. For the representativeness of the relation between *n* and other factors, analysis was done at a larger spatial scale with different climate conditions by combining data from 26 global large basins (~~Figure~~Fig. ~~3~~4).

–<Figure 4 here please>

The correlation coefficient (*r*) between SI and optimized *n* was -0.34 (~~Figure~~Fig. ~~3a~~4a). If the asynchrony of seasonal *P* and $E_0$ was considered in SI, i.e., SAI, the correlation coefficient increased obviously~~,~~ with *r* of -0.51 (Fig. 4b).~~increased to 0.68 (Figure 3b).~~ To further assess the impact of SAI on the fluvial water balance, we also analyzed the roles of SAI in Budyko framework~~ and climate elasticity (Figure 3e, Figure 5)~~. As shown in ~~Figure~~Fig. ~~3~~4e, a larger

~~value of~~ $n$ value was related to a higher evapotranspiration ratio for a given aridity index, and as SAI increased, the value of controlling parameter $n$ tended to decrease. In other words, catchments with a larger SAI had a lower evapotranspiration ratio given the same aridity index. This result is similar to the finding ~~from~~by Zhang et al. (2015), who found that a larger snow ratio caused a higher runoff index ~~for a~~ given dryness index. In contrast, this relationship is not distinct for SI (~~Figure~~Fig. ~~3~~4d). In addition, ~~the accuracy of simulated $n$ using SAI as a predictor was higher than that using SI, i.e., $R^2$ was 0.46 for the former compared to 0.22 for the latter (Figure 4a and 4b).~~ the SAI can explain 51% of the annual variance of parameter $n$, while the SI just explains 22% (Fig~~ure~~s. 4a and 4b). In short, although SI showed a significant relationship with $n$, SAI considering both seasonality and asynchrony of $P$ and $E_0$ was more applicable to represent the difference between water and energy, and better performed in the simulation of $n$ in the Budyko model.

<Figure ~~4~~ 5 here please>

~~To further assess the impact of SAI on the fluvial water balance, we also analyzed the roles of SAI in Budyko framework and climate elasticity (Figure 3c, Figure 5). As shown in Figure 3c, a larger value of $n$ was related to a higher evapotranspiration ratio for a given aridity index, and as SAI increased, the value of controlling parameter $n$ tended to decrease. In other words, catchments with a larger SAI had a lower evapotranspiration ratio given the same aridity index. This result is similar to the finding from Zhang et al (2015), who found that a larger snow ratio caused a higher runoff index for a given dryness index. In contrast, this relationship is not distinct for SI (Figure 3d).~~

The variation of SAI is also ~~plays a role in the~~ sensitive to climate variability~~sensitivity~~. As shown in Fig. 6, ~~Figure 5 shows the spatial patterns of climate elasticities and their relationship with SAI. T~~the climate elasticities of evapotranspiration to precipitation and parameter $n$ ~~to evapotranspiration~~ increased with SAI, whereas the elasticity of evapotranspiration to potential evapotranspiration ~~to evapotranspiration~~ decreased with SAI ~~(Figure 5)~~, which implies ~~, implying~~ that the variation of evapotranspiration in the catchments with a higher SAI were more sensitive to the changes of precipitation and parameter $n$, but less sensitive to the changes of potential evapotranspiration.

<~~Figure~~Fig. ~~5~~ 6 here please>

## 4.2 A semi-empirical formula for parameter ~~n~~ *n*

Previous studies have found that vegetation cover is closely related to the spatial variation of $n$ in different regions (e.g., Li et al. 2013). However, the new finding in this study is that vegetation dynamics (M) also ~~has~~ have a significant impact on the temporal variation of annual values of parameter $n$ (~~Figure~~Fig. ~~3c~~4c; ~~Figure~~Fig. ~~4c~~5c) and evapotranspiration ratio (~~Figure~~Fig. ~~3f~~4f). ~~As shown in Figure 4c, M can explain 67% of spatiotemporal variance of annual $n$ with $MAE$ of 0.28.~~ Nevertheless, the simulation accuracy of $n$ can be further improved, particularly at the high end. As mentioned above, SAI has a significant impact on the variation of $n$. Therefore, based on the results obtained by Li et al. (2013), it is possible to develop a more dynamic model to capture the spatiotemporal variation of parameter $n$, and improve the simulation of $n$ by incorporating SAI into the empirical model.

Following the phenomenological considerations and the relationships demonstrated in ~~Figure~~Figs~~.s~~ ~~3b~~ 4b and ~~3c~~4c, the limiting conditions of SAI and M were achieved: (1) If $\mathrm{SAI} \rightarrow +\infty$, which indicates that the match of $P$ and $E_0$ tends to be the worst, and thus $R \rightarrow P$ and

$E \to 0$, i.e., $n \to 0$; (2) When $\mathrm{M} \uparrow$, then $E \uparrow$, which has been demonstrated by previous studies (i.e., Yang et al., 2009; Li et al., 2013), and thus $n \uparrow$, which can also be found in Figs.~~ures.~~ ~~3e~~ 4c and ~~3f~~4f. Based on these limiting conditions, a semi-empirical formula (SEF) for parameter *n* was obtained as:

$$n = a\mathrm{SAI}^{b}\mathrm{M}^{c} \qquad (13)$$

where *a* and ~~*b*~~ *c* are positive regression coefficients and ~~*c*~~ *b* is negative. Nonlinear least squares can be used to estimate the values of *a*, *b*, and *c*, based on *n* calibrated from measured data. Then, the final equation was as follows

$$n = 0.27\mathrm{SAI}^{-0.30}\mathrm{M}^{0.90} \qquad (14)$$

As shown in ~~Figure~~Fig. ~~4d~~5d, the simulated *n* calculated by ~~semi-empirical formula~~SEF match well with the optimized *n* with $R^2$ of ~~0.82~~0.75 and *MAE* of 0.24. In addition, the E~~e~~q. (13) has also been verified in each catchment among the 26 basins (Table S1). The RMSE and MAE for each catchment is relatively small~~,~~ with ~~the~~ mean values of 12.0 and 14.8 mm, respectively. Except for basins 3, 5 and 26, the $R^2$ values for simulation of *R* in each catchment are larger than 0.5. These results indicated that the M and SAI~~,~~ as well as the semi-empirical formula~~,~~ can well explain the variability of the controlling parameter *n*.

In addition to the ~~semi-empirical formulae~~SEF, ~~multiple~~ linear regression ~~(MLR)~~ is often applied to simulate *n*. For example, taking NDVI, latitude, and topographic index as explanatory variables, Xu et al. (2013) applied multiple linear regression ~~MLR~~ to estimate the spatial variation of *n* for the global large river basins. Considering the multicollinearity ~~problems~~issue, the partial least square regression (PLSR) was used in this study. ~~Accordingly, we also fitted parameter *n* by MLR.~~ As shown in ~~Figure~~Fig. ~~4e~~5e, the values of ~~$R^2$~~ *NSE* and

MAE of the simulated $n$ by using ~~*MLR*~~ PLSR were 0.~~72~~65 and 0.~~23~~27~~,~~ respectively, which was not as good as the performance of the semi-empirical formulae. Therefore, the SEF~~semi-empirical formula~~ was a better choice not only for simulation but also for explaining the physical meaning.

Cross-validation was used to validate the semi-empirical equation. The dataset for one basin was used for validation, and the dataset for the remaining 25 basins were used for calibration. Then the cross-validation process is repeated 26 times, with each of 26 basins used once as validation. Parameter $n$ for the validation basin was simulated by the semi-empirical formula obtained from the other 25 basins. The calibrated parameters for each basin can be found in Table S2~~ in the Supplement~~. Subsequently, based on annual $P_e$, $E_0$ and simulated annual parameter $n$, simulated annual $R$ and $E$ were calculated using ~~eq.~~Eq. (2). The simulated annual $R$ and $E$ for each validated ~~validation~~ basin ~~were~~was combined to compare with the observed $R$ and $E$, respectively (Fig. 7). As shown in ~~Figure~~Fig. ~~6~~7a-b, the simulated annual $R$ and $E$ that estimated by Budyko model with cross-validation parameter $n$ showed a remarkable agreement with the observed ones with ~~$R^2$~~ *NSE* larger than 0.~~96~~ 89 and MAE smaller than ~~35~~ 50.52 mm, which is close to the simulation accuracy of these estimated by Budyko model with simulated parameter $n$ by using the semi-empirical formula (i.e., Eq. (14) (Fig. 7c-d). These results indicated that the semi-empirical formula expressed the spatiotemporal variation of parameter $n$, and the proposed ~~eq.~~Eq. (2) with simulated parameter $n$ was reliable for the simulation of annual $R$ and $E$.

<Figure 7~~6~~ here please>

### 4.3 Contributions of SAI and other factors to R and E changes

To further assess the impact of SAI on the water balance, here we quantified the contributions of SAI and other factors, i.e. $P_e$, $E_0$ and M, on the ~~variation~~ changes of $R$ and $E$ before and after changepoint ~~(Figures 7 and 8)~~.. We used Ordered clustering test, Pettitt test method and AMOC method to detect the change points of $R$. To avoid possible uncertainty within results based on the individual method, the assembled change points were confirmed with more than one method. If the results for all the three methods are different, the median change point would be selected (Liu et al., 2017a). Based on the changepoints of $R$ and the changes rates of $P_e$, $E_0$, M and SAI before and after change points (Table S3 ~~in the supplement~~), the contributions of these four factors to $R$ and $E$ were assessed (Figures 8 and 9; Table S3).

As can be seen from ~~Figures~~Figs. ~~7a~~ 8a and ~~7c~~8c, the $P_e$ changes controlled the variation of $R$ in most basins, with 18 of the 26 selected basins. The absolute value of contributions of $P_e$ changes to $R$ changes ranged from 11% to 96% with the median value at 61% for the 26 basins (Fig ~~7b~~8b). In addition to the $P_e$ changes, the SAI change was also an important factor for the $R$ change with the median absolute contribution at ~~15~~16%. SAI was the dominant factor with the maximum contribution to $R$ changes in six rivers, such as Yangtze, Yellow, Aral, Northern Dvina, Congo and Mississippi basin. The $E_0$ changes reduces the $R$ in ~~most river basins, with~~ 24 of the 26 basins (Table S4). The $E_0$ changes had a limited impact on the $R$ changes with the median absolute contribution of 8%. However, it is the dominant factor for $R$ changes in Parana ~~Danube~~ River basins.

<Figures ~~7~~ 8 and ~~8~~ 9 here please>

The dominant factors of $E$ changes were different from those of $R$ changes (~~Figure~~Fig. ~~8~~9).

Both the SAI and M changes had remarkable impacts on the $E$ changes, which were the dominant factors for the $E$ changes within eight and five basins, respectively. Also, the contributions of SAI and M changes to $E$ changes were larger than those to $R$ changes with the median absolute contributions of 21~~19~~% and ~~21~~28%, respectively. Accordingly, the contribution of $P_e$ to $E$ changes was weaker than that to $R$ changes, the median of which dropped from 61% to ~~35~~32%.

In summary, $P_e$ was the key controlling factor for $R$ and $E$ in most river basins. SAI was the dominant factor for both $R$ and $E$ mainly in East Asian subtropical monsoon zones because of the monsoon variability (Cook et al., 2010), such as Yangtze and Yellow River basins. SAI, M and $E_0$ have larger impacts on the $E$ changes than $R$ changes do, while $P$ has~~ve a more~~ stronger impacts on $R$ changes than $E$ changes do.~~M was the dominant factor for both $R$ and $E$ in temperate maritime climate of Europe, i.e., Danube River basin.in the temperate grassland zone of South America, i.e., Parana River basin. $E_0$ had a limited impact on both $R$ and $E$, but it is the dominant factor for both $R$ and $E$ changes in temperate maritime climate of Europe, i.e., Danube River basin.~~

## 5. Discussion

It has been found that both vegetation coverage and climate seasonality have impacts on water balance (Chen et al., 2013; Li et al., 2013; Zeng and Cai, 2016; Abatzoglou and Ficklin, 2017; Ning et al., 2017; Zhang et al., 2016a). Li et al. (2013) found that long-term vegetation coverage was closely related to the spatial variation of the calibrated parameter of the Budyko model in global river basins. However, vegetation dynamics also influenced the temporal variation of parameter *n*, but the relationship remained to be verified over a larger spatial range (Zhang et al., 2016c; Ning et al., 2017). Results of this study confirmed that the vegetation dynamics had a significant impact on both spatial and temporal variations of the controlling parameter *n* at the global scale.

The seasonality index represents the amplitude difference of seasonal *P* and $E_0$, but does not include the phase difference of seasonal *P* and $E_0$. Investigating the water balance across the Loess Plateau in China, Ning et al. (2017) found that seasonal index, SI, was closely related to the controlling parameter. In this study, however, SI showed a worse correlation with the variation of *n* in the 26 large global river basins than those in Loess Plateau. All catchments selected by Ning et al. (2017) were in the monsoon climate zone, where water and energy are strongly coupled, so the seasonality of *P* and $E_0$ in most catchments was in the same phase. Hence, the asynchrony of water and energy was nonexistent and had a limited impact on the variation of *n*. In contrast, the basins selected in this study covered a large spatial scale with a wide range of climate types. Most basins had different phases between seasonal *P* and $E_0$, such as the Northern Dvina with the phase differences larger than two months. The amplitude difference between seasonal *P* and $E_0$ cannot adequately represent the difference between water and energy in the basins with out-of-phase *P* and $E_0$ (Hickel and Zhang, 2006). In this case, SAI, considering both amplitude and phase differences between seasonal of *P* and $E_0$, was proposed to reflect the difference between water and energy. Results showed that the proposed SAI had a significant impact on *n* and evapotranspiration radio, as well as the sensitively of evapotranspiration to the variation of precipitation, potential evapotranspiration, and catchments characteristics. SAI can also be applied to other studies on water-energy balance.

In small-size catchments, interactions between climate variability, vegetation dynamics, and water balance are more complex (Li et al., 2013). Many other factors, such as basins area, latitude, slope gradient, compound topographic index, and so on (Abatzoglou and Ficklin, 2017; Xu et al., 2013; Yang et al., 2009), have been identified to play a role in the spatial distribution of $n$ for small-size catchments. However, in this study, these factors had little changes at the annual time scale, so they were not considered in determining the annual variation of $n$. This study demonstrated that SAI and M play an important role in the spatiotemporal variation of $n$ in large river basins, nevertheless, other factors should also be considered in the simulation of spatial variation of $n$ for small-size catchments.

SAI was identified to have a great influence on the changes of $R$ and $E$. Especially, the changes of both $R$ and $E$ for the two major rivers (i.e., Yangtze and Yellow River basins) in East Asian monsoon zone is mainly controlled by SAI. Hoyos and Webster, (2007) found that the variation of monsoon systems remarkably affects the climate seasonal pattern (Hoyos and Webster, 2007). Using the covariance of $P$ and $E_0$ as an explanatory variable, Zeng and Cai (2016) indicated that the seasonality of $P$ and $E_0$ had a significant impact on the $E$ variation, such as the Yangtze River basin. Their results are generally consistent with ours. To assess the impact of ecological restoration on runoff in the Loess Plateau of China, Liang et al. (2015) regarded the ecological restoration, i.e., vegetation dynamics, as the cause of changes in $n$. However, our results showed that SAI also played an important role in the changes of $n$, particularly for the East Asian subtropical monsoon zone.

~~$E_0$ is the mainly controlling factor for the changes of both $R$ and $E$ in Danube river. The increased air temperature (Busuioc et al, 2010) increase the potential evapotranspiration~~

~~significantly for the Danube river, which make a deficit increase and a decrease of excess water from precipitation (Bandoc et al., 2012). As a result, the *R* and *E* in Danube river was significantly affected by the $E_0$.~~

Although SAI combined with M can well capture the changes of *n* (~~Figure~~Fig. ~~4d~~5d), the impact of other factors represented by parameter *n* on the water balance not only includes SAI and M, but also the human influence, which has been verified by our previous study (Liu et al., 2017a). As a result, this may cause uncertainty in our findings. The human influences on *R* and *E* need to be further investigated.

## 6. Conclusions

In this study, a semi-empirical formula was developed to simulate the spatiotemporal variation of the controlling parameter *n* in the Budyko model. Influences of climate-vegetation factors on water balance were evaluated. The Choudhury-Yang equation modified by the effective precipitation is recommended to calibrate the controlling parameter *n* and to simulate evapotranspiration (*E*) and runoff (*R*), and their variation.

A climate seasonality and asynchrony index, i.e., SAI, is proposed to reflect the difference between water and energy. Results show that the optimized *n* has a much higher correlation with SAI than the existing SI, implying that the phase mismatch between seasonal water and energy should be considered in the impact assessment of water balance. In general, our results suggest that the catchments with a larger SAI usually have a larger evapotranspiration ratio given the same climatic and underlying condition, and the variation of evapotranspiration tends to be more sensitive to the changes of precipitation and landscape properties (parameter *n*), whereas less sensitive to the potential evapotranspiration in the catchments with larger SAI. Furthermore, this study confirms that vegetation dynamics (M) also plays an important role in modifying the temporal variation of $n$ at the annual scale. Based on SAI and M, a semi-empirical formula for the spatiotemporal variation of parameter $n$ has been developed, and it performs well in the prediction of annual evapotranspiration and runoff.

Employing the developed semi-empirical formula, the contributions of SAI and M, as well as $P_e$ and $E_0$, to the variation of $E$ and $R$ were assessed. Results show that precipitation is the first-order control on the $R$ and $E$ changes, and, secondly, SAI was found to control the changes of $R$ and $E$ in the subtropical monsoon regions of East Asian. SAI, M and $E_0$ have large impacts on $E$ than on $R$, whereas $P_e$ has larger impacts on $R$.

The study assesses the influence of climate variability and vegetation dynamics on water balance, which highlights the role of climate seasonality and asynchrony as well as vegetation dynamics in the annual variation of $n$, and sheds new light on the difference in the contributions of climate-vegetation factors to the changes in $R$ and $E$. This study can be useful for water-energy modelling, hydrological forecasting, and water management.

**Acknowledgments**: This work is financially supported by the National Science Foundation for Distinguished Young Scholars of China (Grant No.: 51425903), the Fund for Creative Research Groups of National Natural Science Foundation of China (Grant No.: 41621061), National Natural Science Foundation of China (No. 41771536), and by Key Project of National Natural Science Foundation of China (Grant No.: 51190091), National Natural Science Foundation of China under Grant No. 41401052, National Key Research and Development Program of China

(Grant No. 2018YFA0605603) and Fundamental Research Funds for the Central Universities, China University of Geosciences (Wuhan) (Grant No. CUGCJ1702, CUG180614). We would like to thank Ming Pan (mpan@princeton.edu), Dan Li (danl@princeton.edu) at Princeton University and Xianli Xu (xuxianliww@gmail.com) at Chinese Academy of Sciences for sharing basin data set. Our cordial thanks should be extended to Dr. Tingting Ning (ningting2012@126.com) from University of the Chinese Academy of Sciences for his professional suggestions. Information of the data were provided with great details in the Data section and further message concerning data please write to zhangq68@bnu.edu.cn. The last but not the least, our cordial gratitude should be extended to the editor and anonymous reviewers for their professional comments and suggestions which are greatly helpful for further quality improvement of our manuscript.

**References**

Abatzoglou, J. T., and Ficklin, D. L.: Climatic and physiographic controls of spatial variability in surface water balance over the contiguous United States using the Budyko relationship, Water Resour. Res., 10.1002/2017wr020843, 2017.

Arnell, N. W., and Gosling, S. N.: The impacts of climate change on river flow regimes at the global scale, J. Hydrol., 486, 351-364, 2013.

~~Bandoc, G.: Estimation of the annual and interannual variation of potential evapotranspiration, Evapotranspiration-Remote Sensing and Modeling, InTech, 251-272, 2012.~~

Berghuijs, W. R., & Woods, R. A.: A simple framework to quantitatively describe monthly precipitation and temperature climatology, Int. J. Climatology, 36(9), 3161-3174, 2016.

Biswal, B.: Dynamic hydrologic modeling using the zero-parameter Budyko model with instantaneous dryness index, Geophys. Res. Lett., 43, 9696-9703, 10.1002/2016gl070173, 2016.

Buermann, W.: Analysis of a multiyear global vegetation leaf area index data set, J. Geophys. Res.-Atmos., 107, 10.1029/2001jd000975, 2002.

Busuioc,A; Caian, M.; Cheval, S.; Bojariu, R.; Boroneant, C.; Baciu, M.; Dumitrescu, A.: Climate variability and change in Romania, Ed. ProUniversitaria, 59-72, ISBN 978-973-129-549-7, București, România 2010.

Cai, D., Fraedrich, K., Sielmann, F., Guan, Y., Guo, S., Zhang, L., and Zhu, X.: Climate and vegetation: An ERA-interim and GIMMS NDVI analysis, J. Climate, 27, 5111-5118, 2014.

Chen, X., Alimohammadi, N., and Wang, D.: Modeling interannual variability of seasonal evaporation and storage change based on the extended Budyko framework, Water Resour. Res., 49, 6067-6078, 10.1002/wrcr.20493, 2013.

Choudhury, B.: Evaluation of an empirical equation for annual evaporation using field observations and results from a biophysical model, J. Hydrol., 216, 99-110, 1999.

Cook, E. R., Anchukaitis, K. J., Buckley, B. M., D'Arrigo, R. D., Jacoby, G. C., and Wright, W. E.: Asian monsoon failure and megadrought during the last millennium, Science, 328(5977), 486-489, 2010.

Dagon, K., and Schrag, D. P.: Exploring the effects of solar radiation management on water cycling in a coupled land–atmosphere model. J. Climate, 29, 2635-2650, 2016.

Donohue, R. J., Roderick, M. L., and McVicar, T. R.: Roots, storms and soil pores: Incorporating key ecohydrological processes into Budyko's hydrological model, J.

Hydrol., 436-437, 35-50, 10.1016/j.jhydrol.2012.02.033, 2012.

Fu, B. P.: On the calculation of the evaporation from land surface, Sci. Atmos. Sin., 5, 23-31, 1981 (in Chinese).

Gentine, P., D'Odorico, P., Lintner, B. R., Sivandran, G., and Salvucci, G.: Interdependence of climate, soil, and vegetation as constrained by the Budyko curve, Geophys. Res. Lett., 39, n/a-n/a, 10.1029/2012gl053492, 2012.

Greve, P., Gudmundsson, L., Orlowsky, B., and S. I. Seneviratne: The Budyko framework beyond stationarity, Hydrol. Earth Syst. Sci. Discuss, 12, 6799–6830, 2015.

Gutman, G., and Ignatov, A.: The derivation of the green vegetation fraction from NOAA/AVHRR data for use in numerical weather prediction models, Int. J. Remote Sens., 19, 1533-1543, 1998.

Hickel, K., and Zhang, L.: Estimating the impact of rainfall seasonality on mean annual water balance using a top-down approach, J. Hydrol., 331, 409–424, 2006.

Hoyos, C. D., and Webster, P. J.: The role of intraseasonal variability in the nature of Asian monsoon precipitation, J. Climate, 17, 4402-4424, 2007.

Koster, R. D. and Suarez, M. J.: A simple framework for examining the interannual variability of land surface moisture fluxes, J. Climate, 12, 1911-1917, 1999.

Legates, D. R., and McCabe, G. J.: Evaluating the use of “goodness-of-fit” measures in hydrologic and hydroclimatic model validation, Water Resour. Res., 35, 233-241, 1999.

Li, D., Pan, M., Cong, Z., Zhang, L., and Wood, E.: Vegetation control on water and energy balance within the Budyko framework, Water Resour. Res., 49, 969-976, 10.1002/wrcr.20107, 2013.

Liang, W., Bai, D., Wang, F., Fu, B., Yan, J., Wang, S., Yang, Y., Long, D., and Feng, M.: Quantifying the impacts of climate change and ecological restoration on streamflow changes based on a Budyko hydrological model in China's Loess Plateau, Water Resour. Res., 51, 6500-6519, 2015.

Liu, J., Zhang, Q., Singh, V. P., and Shi, P.: Contribution of multiple climatic variables and human activities to streamflow changes across China, J. Hydrol., 545, 145-162, 2017a.

Liu, J., Zhang, Q., Zhang, Y., Chen, X., Li, J., and Aryal, S. K.: Deducing climatic elasticity to assess projected climate change impacts on streamflow change across China, J. Geophys. Res.-Atmos., 2017b.

Milly, P. C. D.: Climate, soil water storage, and the average annual water balance, Water Resour. Res., 30, 2143-2156, 1994.

Ning, T., Li, Z., and Liu, W.: Vegetation dynamics and climate seasonality jointly control the interannual catchment water balance in the Loess Plateau under the Budyko framework, Hydrol. Earth Syst. Sci., 21, 1515-1526, 10.5194/hess-21-1515-2017, 2017.

Pan, M., Sahoo, A. K., Troy, T. J., Vinukollu, R. K., Sheffield, J., and Wood, E. F.: Multisource Estimation of Long-Term Terrestrial Water Budget for Major Global River Basins, J. Climate, 25, 3191-3206, 10.1175/jcli-d-11-00300.1, 2012.

Potter, N. J., Zhang, L., Milly, P. C. D., McMahon, T. A., and Jakeman, A. J.: Effects of rainfall seasonality and soil moisture capacity on mean annual water balance for Australian catchments, Water Resour. Res., 41, 10.1029/2004wr003697, 2005.

Wang, D., and Alimohammadi, N.: Responses of annual runoff, evaporation, and storage change to climate variability at the watershed scale, Water Resour. Res., 48, doi:10.1029/2011WR011444, 2012.

Weiss, M., and Coauthors: Contribution of dynamic vegetation phenology to decadal climate predictability, J. Climate, 27, 8563-8577, 2014.

Woods, R.: The relative roles of climate, soil, vegetation and topography in determining seasonal and long-term catchment dynamics, Adv. Water Resour., 26, 295-309, 2003.

Woods, R. A.: Analytical model of seasonal climate impacts on snow hydrology: Continuous snowpacks. Adv. Water Resour., 32, 1465-1481, doi:10.1016/j.advwatres.2009.06.011, 2009.

Xu, X., Liu, W., Scanlon, B. R., Zhang, L., and Pan, M.: Local and global factors controlling water-energy balances within the Budyko framework, Geophys. Res. Lett., 40, 6123-6129, 10.1002/2013gl058324, 2013.

Yan, J. W. and Coauthors: Changes in the land surface energy budget in eastern China over the past three decades: Contributions of land-cover change and climate change. J. Climate, 27, 9233-9252, 2014.

Yang, D., Sun, F., Liu, Z., Cong, Z., Ni, G., and Lei, Z.: Analyzing spatial and temporal variability of annual water-energy balance in nonhumid regions of China using the Budyko hypothesis, Water Resour. Res., 43, , 10.1029/2006wr005224, 2007.

Yang, D., Shao, W., Yeh, P. J. F., Yang, H., Kanae, S., and Oki, T.: Impact of vegetation coverage on regional water balance in the nonhumid regions of China, Water Resour. Res., 45, 10.1029/2008wr006948, 2009.

Yang, H., Yang, D., Lei, Z., and Sun, F.: New analytical derivation of the mean annual water-energy balance equation, Water Resour. Res., 44~~, n/a n/a,~~ 10.1029/2007wr006135, 2008.

Yang, H., Lv, H., Yang, D., and Hu, Q.: Seasonality of precipitation and potential evaporationanditsimpact on catchment waterenergy balance , Journal of Hydroelectric Engineering, Journal of Hydroelectric Engineering, 31, 54-59, 2012 (in Chinese).

Yang, H., Qi, J., Xu, X., Yang, D., and Lv, H.: The regional variation in climate elasticity and climate contribution to runoff across China, J. Hydrol., 517(517), 607–616, 2014.

Yang, H. B., Yang D. W., and Hu Q. F.: An error analysis of the Budyko hypothesis for assessing the contribution of climate change to runoff, Water Resour. Res, 50, 9620–9629, doi:10.1002/2014WR015451, 2014.

Ye, S., Li, H.-Y., Li, S., Leung, L. R., Demissie, Y., Ran, Q., and Blöschl, a. G.: Vegetation regulation on streamflow intra-annual variability through adaption to climate variations, Geophys. Res. Lett., 42, 10.1002/, 2015.

Zeng, R., and Cai, X.: Climatic and terrestrial storage control on evapotranspiration temporal variability: Analysis of river basins around the world, Geophys. Res. Lett., 43, 185-195, 10.1002/2015gl066470, 2016.

Zhang, D., Cong, Z., Ni, G., Yang, D., and Hu, S.: Effects of snow ratio on annual runoff within the Budyko framework. Hydrol. Earth Syst. Sci., 19, 1977-1992, 2015.

Zhang, D., Liu, X., Zhang, Q., Liang, K., and Liu, C.: Investigation of factors affecting intra-annual variability of evapotranspiration and streamflow under different climate conditions, J. Hydrol., 543, 759-769, 10.1016/j.jhydrol.2016.10.047, 2016a.

Zhang, Q., Liu, J., Singh, V. P., Gu, X., and Chen, X.: Evaluation of impacts of climate change and human activities on streamflow in the Poyang Lake basin, China, Hydrol. Process., 30, 2562-2576, 10.1002/hyp.10814, 2016b.

Zhang, S., Yang, H., Yang, D., and Jayawardena, A. W.: Quantifying the effect of vegetation change on the regional water balance within the Budyko framework, Geophys. Res. Lett., 43, 1140-1148, 10.1002/, 2016c.

Zhou, S., Yu, B., Zhang, L., Huang, Y., Pan, M., and Wang, G.: A new method to partition climate and catchment effect on the mean annual runoff based on the Budyko complementary relationship, Water Resour. Res. 52(9), 7163-7177, 2016.

Table 1. Long-term annual mean meteorological and hydrological characteristics and vegetation coverage (1984-2006) for the 26 large river basins around the world.

| Number | Basins | $P$ (mm) | $E_0$ (mm) | $\Delta S$ (mm) | $E$ (mm) | $R$ (mm) | M | SAI | $n$ |
|---|---|---|---|---|---|---|---|---|---|
| 1 | Amazon | 2173 | 1284 | 6 | 1145 | 1022 | 9.2 | 0.5 | 2.3 |
| 2 | Amur | 411 | 756 | -5 | 282 | 134 | 3.8 | 0.9 | 1.1 |
| 3 | Aral | 255 | 1129 | -22 | 209 | 68 | 2.4 | 0.8 | 0.9 |
| 4 | Columbia | 566 | 916 | -20 | 318 | 268 | 4.7 | 1.9 | 0.9 |
| 5 | Congo | 1371 | 1175 | 9 | 1008 | 354 | 8.8 | 0.2 | 3.3 |
| 6 | Danube | 733 | 742 | -14 | 498 | 249 | 6.7 | 0.7 | 1.8 |
| 7 | Indigirka | 223 | 345 | 6 | 73 | 144 | 2.4 | 1.5 | 0.5 |
| 8 | Indus | 450 | 1315 | -6 | 293 | 163 | 2.5 | 1.3 | 0.8 |
| 9 | Kolyma | 267 | 355 | 6 | 125 | 137 | 2.6 | 1.2 | 0.8 |
| 10 | Lena | 352 | 436 | 4 | 180 | 168 | 3.6 | 1.0 | 0.9 |
| 11 | Mackenzie | 392 | 462 | 2 | 212 | 178 | 4.4 | 1.0 | 1.0 |
| 12 | Mississippi | 776 | 1104 | -3 | 578 | 201 | 6.1 | 0.7 | 1.6 |
| 13 | Niger | 616 | 1958 | -10 | 423 | 202 | 3.2 | 1.5 | 0.8 |
| 14 | Nile | 543 | 1863 | -2 | 421 | 124 | 3.7 | 0.7 | 1.0 |
| 15 | Northern Dvina | 588 | 479 | -10 | 267 | 330 | 6.3 | 0.9 | 1.0 |
| 16 | Ob | 474 | 597 | -2 | 275 | 200 | 4.7 | 1.1 | 1.1 |
| 17 | Olenek | 277 | 370 | -2 | 113 | 166 | 2.5 | 1.3 | 0.7 |
| 18 | Parana | 1242 | 1307 | -14 | 982 | 274 | 8.4 | 0.5 | 2.6 |
| 19 | Pearl | 1424 | 967 | -7 | 627 | 804 | 6.1 | 0.7 | 1.2 |
| 20 | Pechora | 544 | 394 | 2 | 186 | 356 | 3.8 | 0.8 | 0.8 |
| 21 | Senegal | 318 | 2014 | -8 | 284 | 41 | 2.0 | 2.2 | 1.0 |
| 22 | Volga | 568 | 651 | -11 | 354 | 225 | 5.6 | 1.2 | 1.3 |
| 23 | Yangtze | 1000 | 857 | -3 | 378 | 625 | 5.4 | 0.5 | 0.8 |
| 24 | Yellow | 424 | 919 | -5 | 324 | 105 | 3.4 | 0.8 | 1.2 |
| 25 | Yenisei | 430 | 468 | -6 | 227 | 209 | 4.3 | 0.8 | 1.0 |
| 26 | Yukon | 268 | 383 | 16 | 86 | 166 | 3.7 | 1.1 | 0.5 |

## Figure captions

**Figure 1.** Two examples showing the mismatch between long-term monthly precipitation ($P$) and potential evapotranspiration ($E_0$), in terms of (a) seasonal amplitudes ($\delta_P$, $\delta_{E_0}$) and (b) phase shift ($S_P$, $S_{E_0}$).

**Figure 2.** Comparing the observed and simulated monthly precipitation and potential evapotranspiration, using the sine function with fixed phase (i.e., Eq. (4)) and fitted phase (i.e., Eq. (6)). Noted that each point represents one-month data based on the combined dataset from 26 global large basins.

**Figure 3.** Examples of three scenarios for the mismatch between water and energy in terms of the relationship of SAI to 1-DI. (a) SAI smaller than 1-DI, implying $P$ larger than PET in the whole year. (b) SAI smaller than DI-1, implying $P$ small than PET in the whole year. (c) SAI smaller than 1-DI, implying a larger SAI means more surplus of $P$. The shaded areas represent the difference between precipitation and potential evapotranspiration, which equal to $(1-DI)+\mathrm{SAI}\sin\left(\frac{2\pi}{\tau}\frac{t}{12}+\varphi\right)$.

**Figure 4.** Relationship between optimized $n$ and (a) SI, (b) SAI and (c) M. (d-f) Distribution of evapotranspiration ratio ($E/P_e$) as a function of the aridity index ($E_0/P_e$) classified by 26 global large river basins at annual scale. The Budyko curves from the top down are derived from Eq. (2b) with $n$=∞, $n$=5, $n$=2, $n$=1, $n$=0.6 and $n$=0.4, respectively. Noted that each point represents one year based on the combined dataset from 26 global large basins.

**Figure 5.** Optimized (calibrated) $n$ versus simulated $n$ modeled by (a) SI, (b) SAI, (c) M, (d) M and SAI using the semi-empirical formula (SEF, Eq. (14)), and (e) M and SAI using the partial least square regression (PLSR). Noted that each point represents one year based on the combined dataset from 26 global large basins.

**Figure 7.** The climatic elasticity of evapotranspiration to the changing precipitation, potential evaporation and other factors represented by controlling parameter $n$ in the 26 global large river basins, and its

relations with the climate seasonality and asynchrony index (SAI). Noted that each point represents one of the 26 global large basins.

**Figure 8.** Absolute value of contributions to the long-term mean changes of Runoff (before and after changepoint of *R*) from $P_e$, SAI, M and $E_0$ changes. The distribution ranges of Absolute value of contribution for each factor are shown in (b) and the number of basins dominated by each factor with the largest relative contribution is summarized in (c).

**Figure 9.** The same as Figure 8 but for relative contribution to the changes of evapotranspiration.